Tectonophysics 646 (2015) 1–19

Contents lists available at ScienceDirect

Tectonophysics

journal homepage: www.elsevier.com/locate/tecto

Review Article

Tectonic significance of serpentinites

Stéphane Guillot [a,*], Stéphane Schwartz [a], Bruno Reynard [b], Philippe Agard [c], Cécile Prigent [a]

[a] Université Grenoble Alpes, CNRS, ISTerre, F-38041 Grenoble, France
[b] Université de Lyon, Ecole Normale Supérieure de Lyon, CNRS, Université Claude Bernard Lyon 1, F-69342 Lyon, France
[c] University Pierre et Marie Curie Paris VI, CNRS, ISTEP, F-75252 Paris cedex 05, France

ARTICLE INFO

Article history:
Received 18 July 2014
Received in revised form 22 January 2015
Accepted 26 January 2015
Available online 12 February 2015

Keywords:
Serpentinite
Strain localisation
Weakening processes
Ocean
Subduction zone
Strike-slip fault

ABSTRACT

At plate boundaries, where deformation is localized along centimetre- to kilometre-scale shear zones, the influence of serpentinite on tectonic processes is linked to its unique rheological properties. In this paper we review the physical properties of serpentinites and their role in tectonic processes. At the ocean–continent transition, serpentinization weakens the upper mantle layer, promoting strain localization and allowing the normal faults in the distal margin to root at low angle. Similarly, at slow to ultra-slow spreading ridges, serpentinite is potentially very abundant at the seafloor and locally associated with domal structures. Extensional deformation is localized in a ~100 m thick shear zone at the footwall of detachment zones dominated by serpentine derived minerals. Within subduction zone, the depth of decoupling between the mantle wedge and the subducting slab corresponds to the stability depth of serpentine weak mineral. Dehydration of serpentine has also been hypothesized to play an important role in the origin of double seismic zones, however the exact mechanism through which dehydration promotes seismicity remains a matter of debate. During exhumation of high-pressure or ultrahigh-pressure rocks, the opposite trajectories of exhumation and subduction require a decoupling zone within the subducting slab. A serpentinized layer has the potential to become a decoupling zone between the oceanic crust and underlying lithosphere. The buoyancy of serpentinite also likely contributes to eclogite exhumation. Finally, along major strike-slip faults, serpentinites have been associated with fault creep, as well as low fault strength. The presence of serpentinite blocks along creeping segments of active faults worldwide is therefore likely to originate from fluids deriving from the progressive dehydration of the mantle wedge that move such bodies upward.

Contents

* Corresponding author. Tel.: +33 4 76 63 59 08.
E-mail address: stephane.guillot@ujf-grenoble.fr (S. Guillot).

http://dx.doi.org/10.1016/j.tecto.2015.01.020
0040-1951/

1. Introduction

Plate tectonics is driven by tectonic forces originating either from mantle convection, slab pull and ridge push. This results in a combination of ductile flow and frictional resistance in fault zones. Lithospheric thickness is variable, ranging from 5 to 100 km in oceanic domains and up to 350 km in cratonic ones. It is assumed to be stabilized against the convective upper mantle as its temperature (~1250 °C) is just below the melting point of peridotite, dominated by the very high strength constituent olivine mineral (Kohlstedt et al., 1995). At plate tectonic boundaries, the lithosphere is deformed and strain localization occurs at kilometre scale suggesting that the strength of the lithospheric mantle is locally reduced. Whatever the tectonic setting (from ocean-floor to subduction zones), the mode of lithospheric deformation is strongly controlled by its rheological layering, which depends on several parameters: deviatoric stress, geothermal gradient, age and nature of the lithosphere, and occurrence of fluids (Burov and Watts, 2006; Huismans and Beaumont, 2012; Mouthereau et al., 2013). Within the upper mantle, between 1250 and 800 °C, several weakening mechanisms have been suggested, as trace amounts of water in olivine will result in significantly lower creep strength (Karato et al., 1986) or a weakening deformation mechanism switch (Précigout and Gueydan, 2009). At higher water/rock ratio and temperatures below 700 °C, the role of serpentinites in active tectonic processes becomes crucial due to its unique rheological properties. Since the discovery of serpentinites at the Atlantic sea floor (Fig. 1) in the 60's (Aumento and Loubat, 1971; Hess, 1962), there has been a growing interest in the Earth Science community for this common rock (Coleman, 1977; Guillot and Hattori, 2013; O'Hanley, 1996). The purpose of this article is to review the tectonic significance of serpentinites at lithospheric plate boundaries. We will first discuss the origin, the mineralogy and the physical properties of serpentine minerals and then highlight the role of serpentinites in the main active tectonic settings.

2. Serpentine and serpentinite

2.1. Mineralogy

We summarize below the main mineral characteristics of serpentinites and serpentine minerals. For a more thorough mineralogical description, the reader may refer to Evans et al. (2013). Serpentinites are solid rocks consisting mostly of serpentine-group minerals, magnetite and sometimes brucite. Secondary minerals are also common, including talc, calcite and magnesite. Serpentinites result from the hydration of ultramafic rocks (dunite, peridotite and pyroxenite) at low (100 °C) to intermediate (700 °C) temperature (Fig. 2). The overall process of serpentinization can be portrayed by a general reaction of the type:

olivine + enstatite + H_2O = serpentine + magnetite (+H_2).

The structural formula of serpentine minerals is $Mg_3Si_2O_5(OH)_4$. The incorporation of a few percentage of Al is common and stabilizes the serpentine at higher temperature (Ulmer and Trommsdorff, 1995; Wunder and Schreyer, 1997; Bromiley and Pawley, 2003; Hilairet et al., 2006; Padrón-Navarta et al., 2013), while the enrichment in Fe and particularly Fe^{3+} takes place at low temperature in hydrothermal environments (Andreani et al., 2013). The peculiar rheological and geophysical properties of serpentinite are due to the specific crystallography of serpentine minerals. The structural unit of serpentinite is a polar 0.72 nm thick layer in which the Mg-rich trioctahedral sheet (O) is tightly linked to a single tetrahedral silicate sheet (T) on one side. On the other side, T–O layers are attached to the next T–O layers by weak H-bonding. To counterbalance the dimensional misfit between the larger T and O sheets, the layers are locally either curved or flat, which results in different types of serpentine.

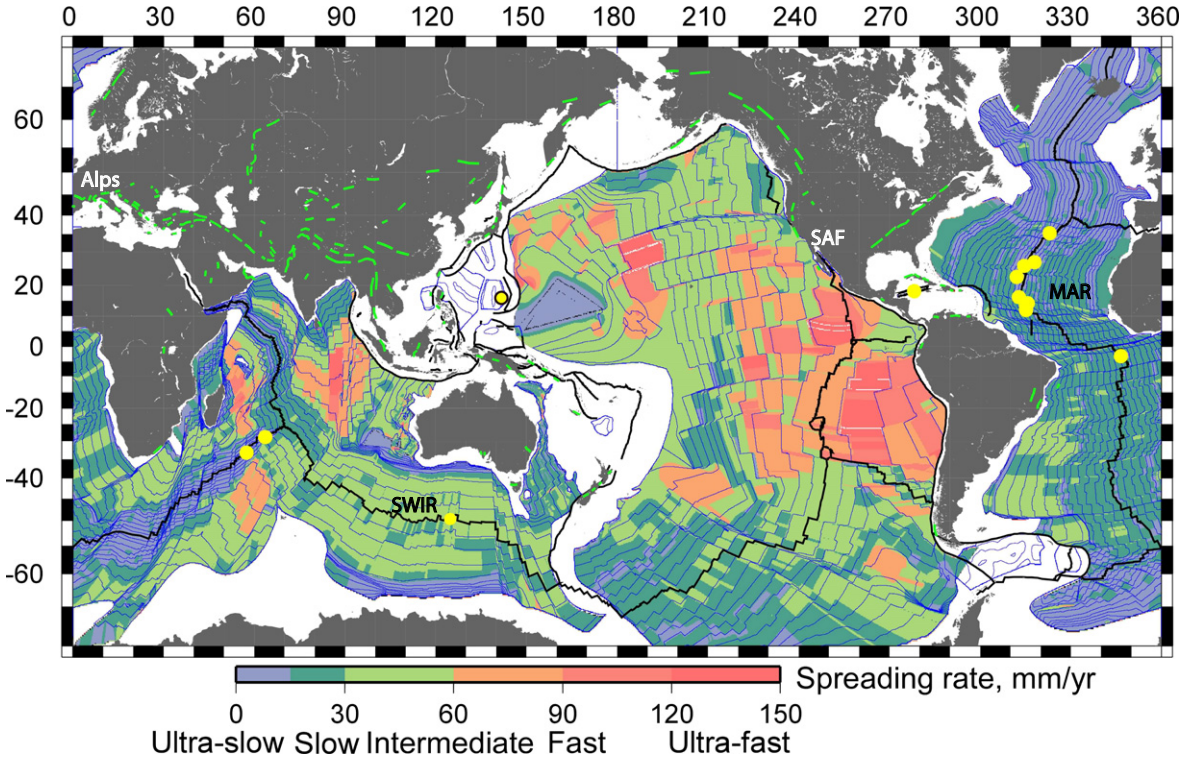

Fig. 1. Map of serpentinite occurrences on the seafloor and continents (modified after Guillot and Hattori, 2013). The oceanic lithosphere is colour coded for spreading rate (Cannat et al., 2010), and the black lines show the ridge axes. The major occurrences of serpentinite are shown by yellow circles for seafloor sites (courtesy of Javier Escartin) and by green lines on continents (based on Coleman, 1971). Serpentinites are also present on the ocean floor in the forearc regions of intra-oceanic, western Pacific arcs (Fryer et al., 1999).

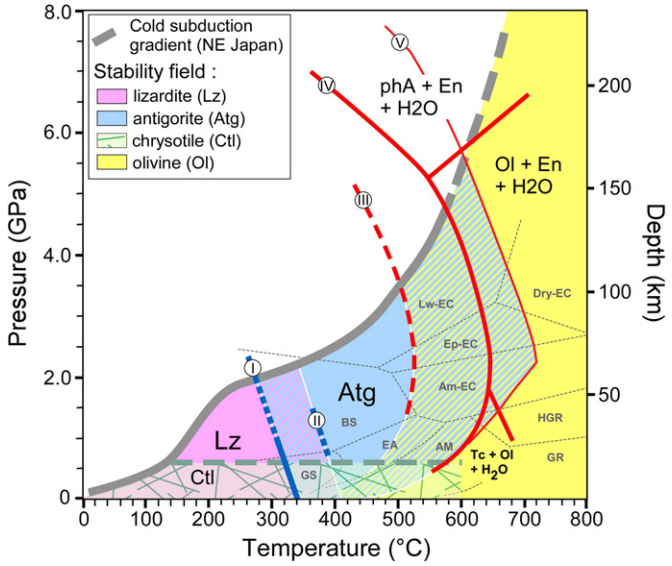

Fig. 2. Pressure–temperature diagram given the stability fields of serpentine species from experimental data and petrological observations in natural serpentinites. (I) Onset destabilization of lizardite into antigorite (Evans, 2004). (II) Maximal stability limit of the lizardite observed in natural serpentinites (Schwartz et al., 2013). (III) Onset of dehydration under water-absent condition (Perrillat et al., 2005). (IV) Stability limit of synthetic antigorite in MSH system (Wunder and Schreyer, 1997). (V) Antigorite breakdown curve (Ulmer and Trommsdorff, 1995). Metamorphic facies boundaries (Liou et al., 2000) and the cold subduction gradient are indicated. This diagram shows the presence of large domain where serpentine species coexist (hatched area) while chrysotile appears into veins.

Lizardite has a flat crystal structure in which the misfit is compensated by coupled substitutions of Mg and Si by Al and Fe^{3+}. Lizardite is the most common mineral in the mesh cells pseudomorphing olivine (Fig. 3a).

Chrysotile forms nanotubes with a central hole. The chrysotile fibre can reach several centimetres in length with an external diameter <100 nm. Chrysotile is poor in Al and Fe^{3+} and mainly fills microfractures that secondary crosscut the rock (Fig. 3a).

Antigorite is composed of curved wavy layers. The O sheet is continuous and wavy whereas the T sheet is periodically reversed along the a-axis, so that it is connected to the concave half-waves of adjacent O sheets (Capitani and Mellini, 2004). The reversals allow antigorite layers to be strongly tied together by covalent Si–O bonds. This explains the lack of easy cleavage (Fig. 2), its higher strength and the different seismic properties of antigorite compared to lizardite and chrysotile (see Reynard, 2013 for review). Antigorite is enriched in Al, Fe^{3+} and Si. Some other microstructures have been observed such as polygonal, polyhedral, and conical serpentines (e.g. Evans et al., 2013) but their scarcity makes them more interesting for mineralogy than for tectonic processes.

Serpentine minerals are stable under a wide range of temperatures and pressures, from the earth surface, hot hydrothermal systems down to subduction environments (Fig. 2). Lizardite and chrysotile are stable at low-pressure low-temperature conditions (0–300 °C, P < 1.0 GPa). Lizardite is usually more stable than chrysotile but chrysotile becomes more stable than lizardite at high water/rock ratio, especially in cleft systems (Evans, 2004). Antigorite is the high-pressure high-temperature stable serpentine. Both experimental and natural constraints (Evans, 2004; Schwartz et al., 2013) show that the lizardite to antigorite transition starts at about 320 °C at a relatively high-pressure (>0.7 GPa) with a complete crystallization of antigorite at temperatures around 390 °C. The onset of antigorite breakdown then occurs at about 460 °C, with a complete destabilization between 650 and 700 °C at 2.0 GPa according to the following reaction (Fig. 2):

antigorite → 18 forsterite + 4 talc + 27 H_2O.

At this pressure, the slope of the antigorite breakdown reaction changes and becomes negative up to 5 GPa and 620 °C (Ulmer and Trommsdorff, 1995). The breakdown of antigorite to forsterite and to Mg-orthopyroxene may produce a large water release at depths of 150 to 200 km in the core of the subducting slab. At the subduction interface, temperatures are high enough to ensure complete antigorite breakdown in a depth range of 70 to 120 km, from the warmest to coolest subduction zones, respectively (Syracuse et al., 2010). The ascent of water into the hot overlying mantle ultimately causes partial melting in the source region for arc magmas (Ulmer and Trommsdorff, 1995; Scambelluri and Phillippot, 2001; Hattori and Guillot, 2003). Chollet et al. (2011) experimentally demonstrated that the antigorite breakdown occurs at a fast rate of 10^{-4} $m^3_{(fluid)}$ $m^{-3}_{(rock)}$ s^{-1}, which is likely much faster than ductile deformation in subduction zones. Fast antigorite breakdown may thus release large amounts of fluids and trigger the observed intermediate depth seismicity (see Section 2.3).

2.2. Rheological properties

Containing up to 13% by weight of OH, serpentine has a low density and the serpentinization process triggers a density drop from ~3.3 to 2.6 g/cm^3 with a concurrent volume increase as large as 40%. The reaction is highly exothermic and rock temperatures can be raised by about 260 °C, thereby providing an energy source for the formation of non-volcanic hydrothermal vents (e.g. Cannat et al., 2010).

Since the seminal work of Raleigh and Paterson (1965), which showed that serpentinite is a weak material and remains ductile even at low temperature, numerous experimental works have been conducted to refine the physical properties of serpentinite and especially its rheology (Morrow et al., 2000 see also Reynard, 2013 for review). However, two main types of uncertainties are associated with estimating the rheological properties of natural rocks: extrapolation of empirical rheological laws (Chernak and Hirth, 2010; Hilairet et al., 2007) from laboratory strain rates (10^{-4} to 10^{-6} s^{-1}) to long-term tectonic strain rates (10^{-13} to 10^{-15} s^{-1}), and sample volumes, which are quite small (mm^3) compared to natural macroscopic shear zones (m^3 to km^3). Despite these technical limitations, some important conclusions arise.

Lizardite, the most common low temperature serpentine is as weak a mineral as micas (Fig. 4), with negligible strain rate dependence (Amiguet et al., 2012; Escartín et al., 1997). At room temperature, Escartín et al. (1997) showed that the transition from brittle to ductile frictional deformation at confining pressure of 200 to 400 MPa is controlled by the development of non-dilatant micro-cracks along one direction within the basal plane [001]. This peculiar mechanical response to stress is easily explained by the mineral structure. As discussed above, lizardite is a phyllosilicate with weak interactions between OH groups and silicate layers and its friction coefficient is relatively low, between 0.3 and 0.5 (Moore et al., 1997; Reinen et al., 1994). This leads to easy gliding along the basal plane with critical resolved shear stress of ca. 100 MPa, and to weak shear zones with basal plane of lizardite in the foliation (Amiguet et al., 2012).

Experimental studies of antigorite have produced apparently contradictory results regarding its deformation behaviour, but antigorite is likely ductile at intermediate temperature and high pressure, especially during seismic events (Figs. 4 and 5) (Auzende et al., 2015; Chernak and Hirth, 2010; Escartin et al., 2001; Hilairet et al., 2007). At low confining pressures, between 0.4 and 1.0 GPa, antigorite, like lizardite, displays a ductile frictional behaviour due to the same process of non-dilatant micro-cracks development (Escartín et al., 1997). It is also associated with minor but perceptible contribution of dislocation gliding along the basal plane (Auzende et al., 2015). The transition from brittle to ductile deformation, and then more distributed deformation, occurs when the bulk sample strength becomes less than the frictional strength (Hirth and Guillot, 2013). At higher pressures, between 1.0 and 4.0 GPa, Hilairet et al. (2007) reported a large strength dependence on

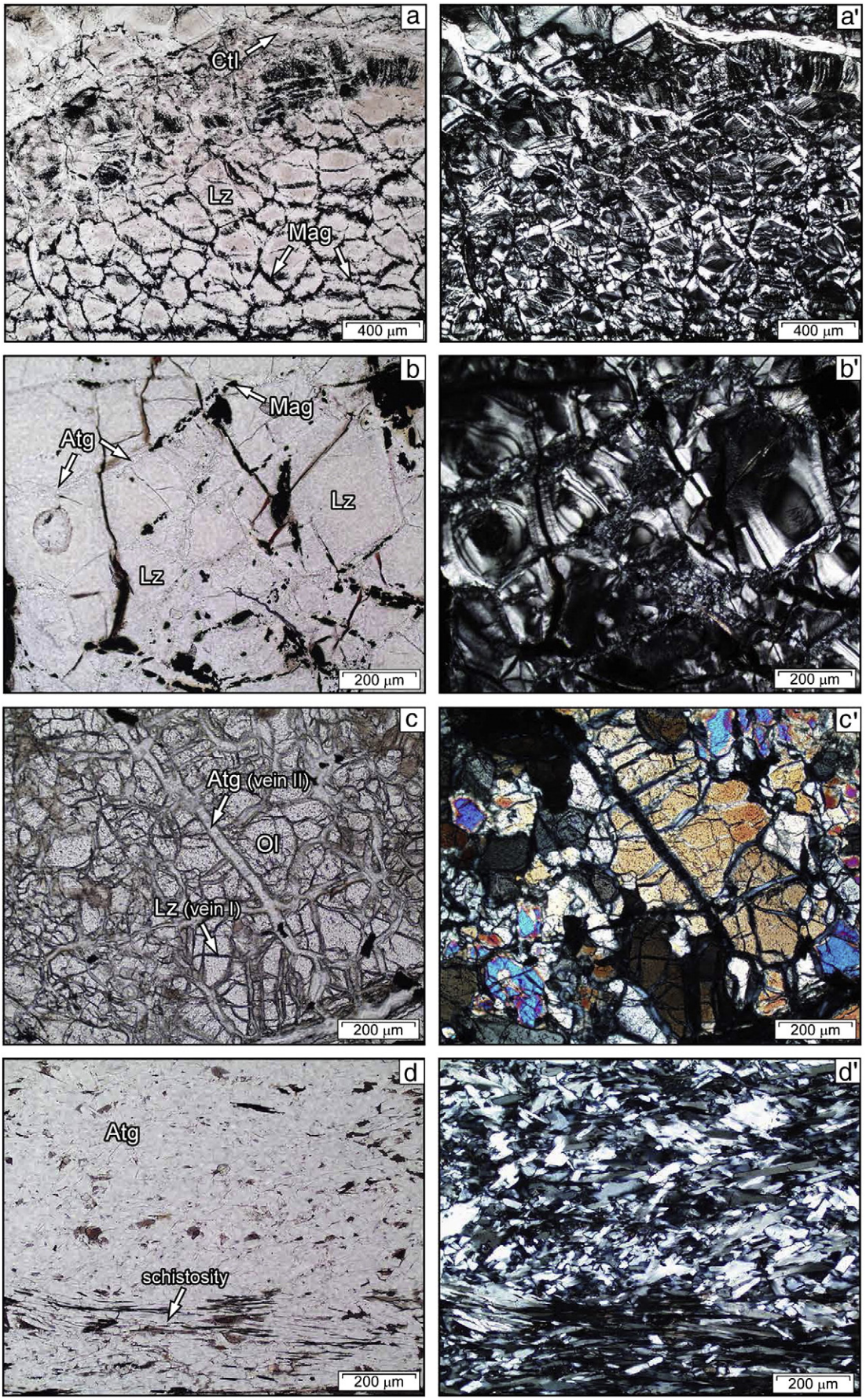
a
Ctl
Lz
Mag
400 μm
a'
400 μm
b
Mag
Atg
Lz
Lz
200 μm
b'
200 μm
c
Atg (vein II)
Ol
Lz (vein I)
200 μm
c'
200 μm
d
Atg
schistosity
200 μm
d'
200 μm

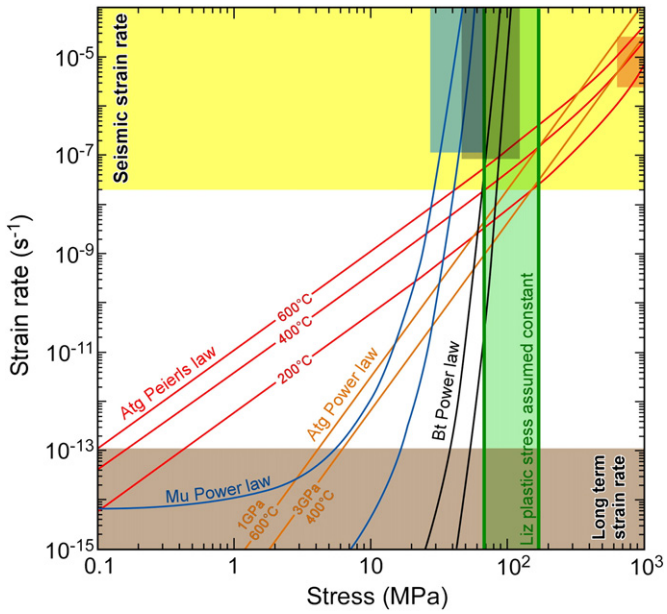

Fig. 4. Rheological behaviour of phyllosilicates (modified after Amiguet et al., 2012). Coloured areas represent experimental dataset in green for muscovite, in grey for biotite and in orange for antigorite. Extrapolation of antigorite (Atg) flow laws using a Peierls law (red curve) calculated for 200, 400 and 600 °C from bottom to top, and a power law (orange curves) calculated for 400 and 600 °C and for two pressures 1GPa and 3GPa. Flow laws for micas are represented in blue for muscovite (Mu) and in black for biotite (Bt) for room T.

strain rate (Fig. 4) with power-law type behaviour ($\dot{\varepsilon} \approx \sigma^3$) (Fig. 5). Chernak and Hirth (2010) reported a similar strength of antigorite at 1.5 GPa as Hilairet et al. (2007), but interpreted it as semi-brittle flow at high pressure, high temperature and elevated strain suggesting a combination of ductile and brittle processes. The authors attributed the transition back to localized behaviour at high temperature to a decrease in the friction coefficient. They also noted a strong dependence of strength on strain rate. According to Reynard (2013 and references therein), this is not inconsistent with a power-law flow given that high stresses of several kbars, leading eventually to failure, can be attained if uncontrolled strain rates in the experiment locally occurred. Jung et al. (2004) also documented faulting of antigorite at 550 °C and 1.5 GPa and Jung et al. (2011) attributed acoustic emissions to faulting and subsequent frictional sliding during pressurization of antigorite up to 6 GPa and 570 °C, but they used elevated strain rates of 10^{-4} s^{-1}. This transition in the deformation mode is also consistent with geological observations showing that whenever serpentinites are involved in large-scale displacements (such as along major strike-slip fault or exhumation of ultra-high pressure rocks) deformation still remains localized in centimetre to hectometre wide shear zones (see Section 3), thereby pointing to an effective ductile flow behaviour (Fig. 6). One should also take into account the fact that foliated serpentinites (Fig. 3d) evidence syntectonic crystal growth and hence a truly plastic deformation at strain rates lower and potentially lower strength than available experimental flow laws. Whatever the mode of deformation, the effective viscosity of serpentinite is much lower (10^{17} to $< 10^{20}$ Pa.s) than the viscosity of the dry upper mantle ($> 10^{22}$ Pa.s; Fig. 5) at geological strain rate (Hilairet et al., 2007; Chernak and Hirth (2010).

Gasc et al. (2011) showed the absence of acoustic emission, thus absence of brittle deformation during high-pressure deformation and dehydration of antigorite. By contrast, Auzende et al. (2015) show that when dehydration occurred in experiments, plasticity increases and is coupled to local embrittlement attributed to hydraulic fracturation due to migration of dehydration fluids, suggesting that dehydration can contribute to intermediate-depth seismicity.

The friction law (μ) of antigorite is sensitive to temperature. At room temperature, μ is relatively high, between 0.5 and 0.85, decreases to 0.4–0.6 between 25 and 194 °C (Moore et al., 1997) and dramatically drops down to 0.1–0.35 at temperatures comprised between 400 and 550 °C (Fig. 5). Moreover, antigorite undergoes a dramatic dynamic weakening ($\mu \approx 0.1$) associated with the onset of dehydration and talc formation at seismic slip velocities above 0.1 m/s (Chernak and Hirth, 2010; Kohli et al., 2011). It is noticeable that talc produced by serpentine dehydration or high silica activity during serpentinization, is one of the weakest minerals (e.g. Escartín et al., 2008 and reference therein) and could partly explain the extreme weakness of talc bearing serpentinite shear zones.

2.3. Geophysical properties

In inaccessible settings where serpentinites are expected, such as subduction zones or oceanic domains, geophysical data is a powerful tool to estimate the degree of mantle serpentinization. It is therefore crucial to know the seismic velocities of serpentinite rocks.

Low seismic velocities, high Vp/Vs ratio and strong S-waves anisotropy characterize serpentine minerals. Chrysotile-dominant serpentinite rocks display very low P-wave velocities down to 4.6 km/s and Vs down to 2 km/s (Carlson and Miller, 2003; Christensen, 2004). These low velocities are due to the large porosity of the chrysotile nanotubes (Reynard, 2013). Pure antigorite displays higher velocities than chrysotile-bearing rocks with Vp in the range of 6.4–6.8 km/s and shear-wave velocities with typical values of 3.5–3.8 km/s (Bezacier et al., 2010a; Christensen, 2004; Hilairet et al., 2007; Horen et al., 1996). P-wave (7.2 km/s) and S-wave (3.8 km/s) velocities of gabbro are quite similar to the wave velocities of partly serpentinized and those rocks can be geophysically indistinguishable (Carlson and Miller, 2004). The Vp/Vs ratio of chrysotile-serpentinites, up to 2.15, is much higher than that of antigorite-serpentinites, which ranges between 1.76 and 1.85 (with a Poisson ratio of ~0.26–0.29, respectively; Bezacier et al., 2010a; Ji et al., 2013).

Considering that Vp/Vs ratio of peridotite and eclogite is ~1.73 (Bascou et al., 2001; Pera et al., 2003), seismological data can only unequivocally differentiate serpentinites from dry mantle rocks in the case of chrysotile-bearing rocks, that is at low pressure. Antigorite-serpentinites in subduction are evidenced by lower seismic velocities (Bezacier et al., 2010a; Reynard, 2013). It is worth noting that gabbros have similar seismic characteristics to serpentinites (Bezacier et al., 2010b) complicating the determination of the Moho depth at slow-spreading ridge (Cannat, 1993).

V anisotropy (A) is defined as: $A = ((Vmax - Vmin)/Vm)$ where Vmax, Vmin, and Vm are, respectively, the maximum, minimum, and mean values of the P or S-wave velocities measured in a given sample

Fig. 3. Photomicrographs of characteristic textures of serpentine species from western Alps and Cuba ophiolites, Atg: antigorite; Lz: lizardite; Ctl: chrysotile, Mag: magnetite; Ol: olivine. x-Polarized light, x′-crossed-polarized light. a–a′. Sample ICH2 Chenaillet ophiolite. Mesh texture after olivine is observed where lizardite is the only developed serpentine species. At the top of the photograph secondary veins infilled by chrysotile crosscut the mesh texture. b–b′. Sample Cu63 base of the Cretaceous arc metamorphosed under greenschist facies conditions. The sample is dominated by mesh texture underlined by lizardite. Locally, secondary antigorite representing few percents of the matrix, is crystallized at the boundary of the lizardite minerals. c–c′. Sample Cu55 slightly serpentinized peridotite collected from the amphibolitic facies serpentinite mélange in the Zaza zone. Olivine grains are well preserved and crosscut by two generations of infilling serpentine veins. The earliest one is composed of lizardite and developed in micro-cracks within the olivine grains (brownish colour). Notice that under crossed-polarized light the lizardite minerals are crystallizing in the same oriented vein and they present the same optical orientation. The second generation of serpentine species corresponds to antigorite. They crystallized exclusively within secondary veins cross-cutting all olivine grains. d–d′. Sample Cu12 was collected from the zoisite-eclogitic facies nappe in the Escambray massif. The matrix is characterized by the development of schistosity underline by the preferred orientation of antigorite minerals.

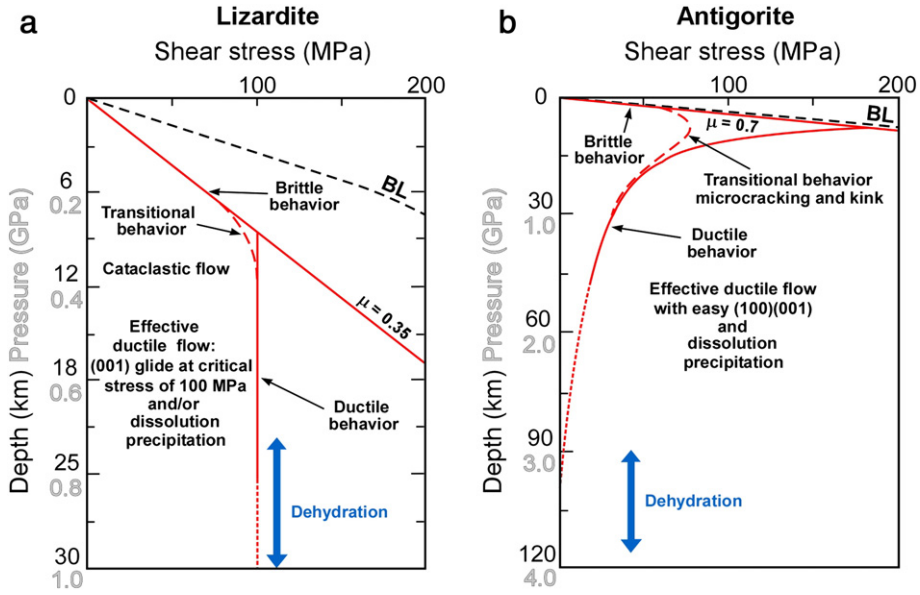

Fig. 5. Yield strength envelope for a) lizardite, and b) antigorite as a function of depth for strain-rate of 10^{-10} s^{-1} (modified after Amiguet et al., 2014).

along three orthogonal propagation directions. The intrinsic anisotropy of the antigorite-serpentinite is likely caused by dislocation creep induced crystal-preferred orientation (CPO) of antigorite along the basal plane (Amiguet et al., 2014). The highest anisotropy (about 40% for Vp and 50% for Vs) was calculated for natural foliated serpentinites (Fig. 3d) having a particularly strong CPO with c-axis perpendicular to the foliation (Van de Moortele et al., 2010). This can be thus considered as an extreme case for seismic anisotropy velocities (Bezacier et al., 2010a). An average value of 10.5% for Vp, and 10.4% for Vs has been observed from a systematic study of Ji et al. (2013). The anisotropy of foliated serpentinites is characterized by the orientation of two fast principal axes in the foliation plane and one slow axis perpendicular to it. This anisotropy pattern is very different from that of peridotites (Pera et al., 2003), in which one fast axis is generally aligned with the lineation and two slow axes are perpendicular to it, corresponding to the so-called A-type olivine fabric. Foliated serpentinites with similar CPO are common in subduction zone (Hirauchi et al., 2010) and in high-pressure terrains (Jung et al., 2011). Another common CPO is

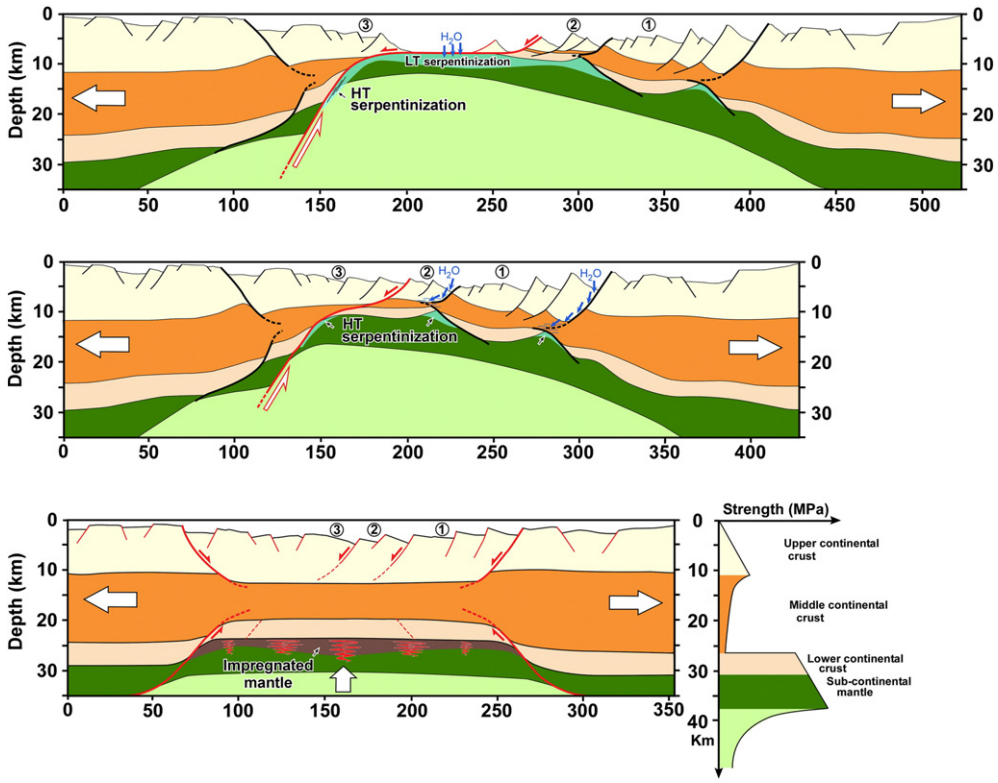

Fig. 6. Dynamic evolution of a hyper-extended continental margin up to the formation of the ocean–continent transition (modified after Mohn et al., 2012; Hirth and Guillot, 2013; Sutra et al., 2013). The hyperextended (≤10 km), continental crust corresponds to a 100 km wide zone of exhumed mantle. Gravimetric and P wave seismic velocities comprised between 5 and 8 km/s show that the degree of serpentinization in this area varies between 15 and 100% and that this zone is about 5 km thick. Below this serpentinized zone, the normal fresh mantle is characterized by P wave velocities above 8 km/s.

with a strong b-axis clustering along the lineation and a perpendicular girdle-like distribution of c-axis (Nishii et al., 2012), which may be partly inherited from topotactic replacement texture during serpentinization (Boudier et al., 2010; Wallis et al., 2011). This results in an orthorhombic anisotropy, not far from a transverse isotropic medium, with one fast and two slow principal axes. This pattern looks similar to that of deformed peridotites, but with a much higher anisotropy along the lineation (shear wave anisotropy of 30% for serpentinite compared with 10% for peridotite; Reynard, 2013). Foliated serpentinites may account for part of the large trench-parallel anisotropy observed in subduction zones (Katayama et al., 2009), and especially for thin layers with highly variable anisotropy at the top of the subducted slabs (Bezacier et al., 2010a; Nikulin et al., 2009).

3. Serpentinites in active tectonic settings

3.1. Serpentinites in OCT and in embryonic oceanic crust

Due to the increase of offshore seismic refraction data at continental passive margins, the terminology of "oceanic to continental boundary", suggesting a sharp contact between the continent and the ocean, is progressively replaced by the term "oceanic to continent transition" (OCT) suggesting instead that this hundred of km wide zone is more complex than initially thought.

Since the discovery of serpentinites along the Iberia margin (ODP Leg 103, Boillot et al., 1980), serpentinites have been found elsewhere, on both sides of the Atlantic margin (ODP Leg 210, Tucholke and Sibuet, 2007), along the South-Australian margin (Nicholls et al., 1981) and in the middle of the Red Sea (Bonatti et al., 1986; Fig. 1). Using seismic data, Minshull (2009) proposed that about 50% of the world magma-poor margins are formed by serpentinized exhumed mantle. Serpentinites have also been recognized in the Alpine–Apenninic ophiolites for a long time (Steinmann, 1905) and are classically interpreted as originating from a slow-spreading ridge system (e.g. Hattori and Guillot, 2007; Lagabrielle and Cannat, 1990). More recently, these ophiolites have also been shown to display clear petrological and tectonic features indicating extension-driven exhumation of the continental mantle at the foot of the Tethyan continental margins (e.g. Deschamps et al., 2013; Manatschal and Müntener, 2009). Similarly, in the Pyrenees, the peridotites from Lherz and the serpentinite massifs disseminated along the North Pyrenean Fault have recently been interpreted as representing the continental mantle exhumed at the OCT (Jammes et al., 2009; Lagabrielle and Bodinier, 2008). According to offshore (Newfoundland and Iberia margins) and onshore (Alpes, Pyrenees) observations, we will summarize here the role of serpentinites at magma-poor margins during the rifting process (Fig. 6).

The OCT corresponds to a ~200 km wide transition zone from a normal thick ($\approx$30 km) then hyperextended ($\leq$10 km) continental crust to a 100 km wide zone of exhumed mantle (Fig. 6). Gravimetric and P wave seismic velocities comprised between 8 and 5 km/s (Minshull, 2009) show that the degree of serpentinization in this area varies between 15 and 100% and that this zone is about 5 km thick. Below this serpentinized zone, P wave velocities above 8 km/s point to the presence of normal, fresh mantle. This system corresponds to a serpentinization front (Canales et al., 2000; Debret et al., 2013; Mével, 2003) where the rheological behaviour of ultramafic rocks depends on the extent of their serpentinization. Above 15% of serpentinization the strength of an altered peridotite is reduced to that of a pure serpentine (Escartin et al., 2001). The 15% serpentinization limit thus represents an important mechanical decoupling layer. Below the hyperextended crust, serpentinized mantle is suspected to extend to about 6 km depth below the top of the basement (Chian et al., 1999; Minshull, 2009). Taking into account a gradual increase of P wave velocities from 7 to 8 km/s, this suggests that the mantle beneath the hyperextended crust contains of a maximum of 75% of serpentinites (recalculated according to Reynard, 2013). Within the exhumed serpentinized mantle and beneath the hyperextended crust, a strong continentward dipping reflection is observed on both sides of rifting margins (Whitmarsh et al., 2001; Hopper et al., 2006; Reston et al., 1996). This S-type reflection or H-reflection is interpreted as the contact between the hyperextended crust and the serpentinized mantle (Reston et al., 1996; Sutra and Manatschal, 2012). This reflector indeed reaches the surface where the continental crust wedges out and the mantle is exhumed at the seafloor (Sutra et al., 2013).

This upper serpentinized mantle is atypical, having intermediate petrological and geochemical characteristics between oceanic and continental mantle, suggesting less than 10% of partial melting and a percolation of mafic melts (Hébert et al., 2001; Péron-Pinvidic and Manatschal, 2009). Indeed, though serpentinized impregnated spinel lherzolites dominate, spinel harzburgites have been drilled in places (Müntener and Manatschal, 2006). Tectonic breccia and semi-brittle gouge composed of gabbro, amphibolite and serpentinite clasts in a calcite-rich or chlorite-rich matrix cataclasite have also been dredged or drilled (Whitmarsh et al., 1998). Skelton and Valley (2000) show, based on oxygen stable isotopes, that the onset of serpentinization associated with gouge formation occurred at temperatures below 300 °C and is dominated by lizardite–chrysotile assemblage. Secondary fluid infiltration of cooler seawater (<100 °C) along normal fault scarps occurs during seafloor exhumation of the serpentinized mantle (Fig. 6).

Long considered as the archetype of a slow-spreading ridge preserved in an orogenic system (e.g. Lagabrielle and Cannat, 1990; Nicolas and Dupuy, 1984), the western Tethyan suture from the Pyrenees, the Alps and the Apennines shows all the petrological and tectonic characteristics of a magma-poor continental margin. The only clear evidence of a preserved oceanic domain in the western Tethyan suture is the Monte Maggiore ophiolite in Corsica, in which depleted mantle is genetically linked to the MORB found in the ophiolitic sequence (Rampone, 2004). All other ultramafic rocks, whether partly (Bodinier and Godard, 2014; Debret et al., 2013; Le Roux et al., 2007; Müntener et al., 2000, 2004, 2010; Piccardo et al., 2004) or fully serpentinized (Deschamps et al., 2012, 2013; Hattori and Guillot, 2007), are comparable to the mantle rocks drilled from the Iberia–Newfoundland OCT and can be summarized as follows. Spinel bearing lherzolites associated with pyroxenites dominate. When clinopyroxenes are preserved, their composition shows that these rocks are equilibrated at relatively low temperature (800 to 950 °C), which is typical of lithospheric conditions. It thus likely represents the continental lithosphere inherited from the late Variscan orogenic events. Locally, such as the Lower Platta unit and in the Lanzo massif, or also in the Apennines, subordinate harzburgites and dunites are associated with serpentinized lherzolites. In this case, spinel lherzolites are impregnated and partly replaced by plagioclase bearing lherzolites. Two pyroxene thermometry on primary minerals indicates higher temperature of equilibration (1200 °C). Isotopic geochronology indicates that magmatic infiltration occurred at the onset of rifting, 165 Ma ago (Kaczmarek et al., 2008; Rampone et al., 1995), prior to mantle exhumation at the seafloor. This suggests that extreme crustal thinning during final rifting was accompanied by melt infiltration at depth (Bodinier et al., 1990; Manatschal and Müntener, 2009). Some exceptional outcrops are found in the Alps (Totalp and Tasna units) and in the Pyrenees (Etang de Lhez) showing the relationship between the continental crust and the exhumed serpentinized mantle on the paleo-seafloor. The exhumed serpentinized mantle is in direct contact with the upper continental crust through a hectometre-scale subhorizontal detachment fault similar to the S-type reflexion from the Iberia margin (Reston et al.;, 1996). This detachment fault has recorded a long and complex history, which can be summarized as follows.

When preserved, peridotites present a foliation underlined by the crystal preferred orientation (CPO) of spinel and olivine porphyroclasts (Le Roux et al., 2007; Müntener et al., 2000). Analysis of microstructures and olivine CPO in harzburgites from the Pyrenees suggests deformation by dislocation creep with the activation of the high-temperature

[100] slip system. The formation of secondary lherzolites and websterites by melt impregnation modifies both the microstructure and the CPO of the harzburgitic protolith: lherzolites show that larger and more equant grains and olivine CPO are quite similar to those in harzburgites, but weaker. The increase in grain size and the dispersion of the olivine CPO in lherzolites through harzburgite–lherzolite contacts may be due to static recrystallization of new randomly oriented olivine crystals during melt-rock reactions (Tommasi et al., 2004). Picazo et al. (2013) described in the Totalp unit (Swiss Central Alps) discrete mylonitic shear zones cross cutting the lherzolite away from the contact with the continental rocks. Mylonites show rounded porphyroclasts of olivine and spinel defining a very fine-grained (2–10 μm) foliation. Similar mylonites and ultramylonites containing high temperature amphiboles have been observed in the Val Malenco (Kaczmarek and Müntener, 2008; Müntener et al., 2000) and in the Voltri massif, NW Italy (Hoogerduijn Strating et al., 1993) suggesting the presence of interstitial melt and/or fluids during deformation (Fig. 6) (Kaczmarek and Müntener, 2008). The same interpretation was proposed for high temperature peridotite mylonites from the Galicia margin (ODP Leg 103; Beslier et al., 1990).

Ultramafic rocks are partly to fully serpentinized and are fractured in metric blocks with no or little displacement. The grain size of the serpentinites decreases towards the top, with smaller centimetre to millimetre angular clasts. The last top ten metres are defined as a core zone with maximum strain (Manatschal and Müntener, 2009; Manatschal et al., 2006), made of a gouge zone containing foliated cataclasite serpentinite. The foliation clearly overprints the pre-existing cataclastic texture. The serpentinite is dominated by lizardite and chlorite showing top to the continent sense of shear. At the contact with the sediments, talc is commonly observed (Lagabrielle et al., 2010; Manatschal et al., 2006) suggesting that silica-rich fluids percolated during shearing. It is also noticeable that the grain size reduction in the serpentinite gouge is marked by a transition from millimetre foliated lizardite to micrometric oval-shaped clasts of chrysotile showing a strong preferred orientation suggesting that strain localization occurred during global cooling of the detachment fault at the ductile to brittle transition (Picazo et al., 2013).

The gouge zone is usually impregnated by secondary calcite, defining the so-called ophicalcite and overlain by tectono-sedimentary breccias that grade into sedimentary breccias and post-rift sediments (Clerc et al., 2012; Florineth and Froitzheim, 1994; Lagabrielle et al., 2010; Lemoine et al., 1987). Lemoine et al. (1987) distinguished two types of ophicalcite. The first type (ophicalcite 1) corresponds to the cataclasite breccia described above, with clasts of lizardite and gabbroic pebbles infilled by calcareous dikes. The first type of ophicalcite is either described at the paleo-seafloor (Lemoine et al., 1987) or within the detachment fault just below the hyperextended continental crust (e.g. Manatschal and Müntener, 2009). The second type of ophicalcites (ophicalcite 2) was deposited above the serpentinite detachment fault and is only observed at the paleo-seafloor (Fig. 7; Decandia and Elter, 1972; Bernoulli and Jenkyns, 1974; Lemoine et al., 1987). This continuous layer is a sedimentary breccia, up to several metres thick, and made predominantly of serpentinite and a few gabbroic pebbles in a chloritic and calcite matrix. It corresponds to debris flows coming from the dismantling of high angle normal fault escarpments (Lemoine et al., 1987) that have been affected by static hydrothermal circulations at the seafloor. Cataclasites and gouges associated with ophicalcites and tectono-sedimentary breccias are widely recognized from mid-ocean ridges (e.g. Boschi et al., 2006; Escartín et al., 2003) and have been drilled along the Iberia–Newfoundland margins (Robertson, 2007) or along the steep Romanche Fracture zone (Bonatti et al., 1974).

3.2. Serpentinites at slow to ultra-slow spreading ridges

The slow to ultraslow spreading ridges (<40 mm/year), represent a total length of 31,880 km and include the Mid-Atlantic Ridge (MAR), the South-West Indian Ridge (SWIR) and the Gakkel Ridge in the Arctic Ocean (Fig. 1). Since their first discovery along the Mid-Atlantic Ridge (Aumento and Loubat, 1971; Hess, 1962), serpentinites have been extensively recognized at slow to ultraslow spreading ridges locally making up to 25% of the seafloor (Cannat et al., 2010; Fig. 1). Available Vp and Vs seismic profiles (Carlson, 2001; Minshull, 2009) suggest, however, that serpentinites may represent only a few percent of slow spreading ridge lithospheres and are abundant near fracture zone only. Serpentinites have also been locally recognized in the Pacific seafloor but those serpentinites are arguably related to subduction activity and will not be discussed in this chapter.

While the volcanic activity is continuous at intermediate to ultra-fast spreading ridges (>60 mm/year.), the volcanic activity at slow to ultra-slow spreading ridges is discontinuous in space and intermittent through time. This favours the production of a heterogeneous crust, in term of both lithology and thickness. The local increase in P-wave velocities, from 5 to 8 km/s at 3–4 km depth, is regarded as characteristic of restricted magmatic activity with a thin crust and a large volume of serpentinites (Canales et al., 2000; Cannat, 1993; Detrick et al., 1993; Dick, 1989). Some P-wave velocity profiles show elsewhere that the first 6–7 km are composed of an association of basalts and gabbros and match normal crustal thickness. Along the MAR axis, where magmatic activity is moderate, serpentinites outcrop off-axis on one side of the ridge at the favour of oceanic core complex (OCC; Tucholke and Sibuet, 2007). OCCs correspond to dome-like shaped massifs, up to 3000 m high above the seafloor (Karson et al., 2006) and usually limited

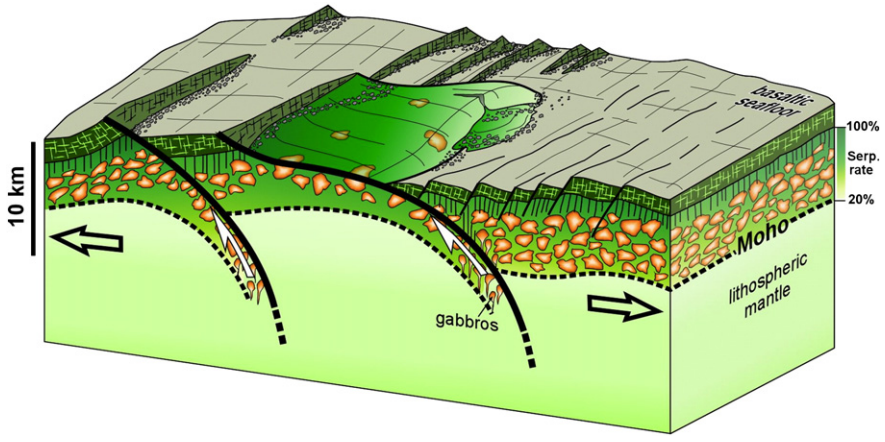

Fig. 7. Schematic 3-D block diagram of an oceanic core complex (OCC) (after Karson et al., 2006; Cannat et al., 2009; Hirth and Guillot, 2013). Notice the development of ophicalcite 2 at the foot of scarp faults.

in size (≈10 × 20 km for the Atlantis massif at 30°N; Fig. 7). OCCs are formed by unroofing of serpentinized mantle and gabbroic crust along low-angle kilometre-scale detachment faults (Fig. 7). Associated lateral displacement exceeds 10 km perpendicular to the axial-valley (Blackman, 2002; Cann et al., 1997). The top of the OCC is marked by a striated surface, also called corrugated surface, created at the footwall of the rolling-hinge active normal fault. This footwall is systematically made of basaltic rocks (Smith et al., 2006). The OCC usually presents a scarp termination dipping towards the ridge axis (Fig. 7). Along the SWIR axis, where the magmatic activity is poor (Fig. 1), OCCs also show corrugated surfaces but some display a smoother transition with the seafloor, without any scarp (Cannat et al., 2009). Finally, in the very poor magmatic area (<3% of gabbro and >97% of serpentinites at seafloor), the morphology of the seafloor is very smooth over a large area, >60 km along the axis (Cannat et al., 2006) and shows rolling-hinge normal faults dipping either on-axis or off-axis (Fig. 7).

The corrugated surface corresponding to the footwall of the major detachment fault has been dredged and drilled at the top of several OCCs along the MAR, at 15°45′N (Bach et al., 2004; Escartín et al., 2003; MacLeod et al., 2002), at 23°21′N (Andreani et al., 2007; Canales et al., 2000; Hansen et al., 2013; Mével et al., 1991), and at 30°N (Atlantis Massif; Blackmann et al., 2002, 2011; Karson et al., 2006; Ildefonse et al., 2007) and shows very similar lithologies and associated tectonic structures. Dominant rock types are serpentinized harzburgites and olivine-bearing gabbros. Serpentinization varies between 50 and 100%, but highly serpentinized peridotites (>80%) dominate in the first hundred metres. The spatial distribution of gabbros and serpentinites is not random. For instance, the northern part of the Atlantis massif is dominated by gabbroic bodies (Blackman et al., 2011) and minor serpentinites are exposed while its southern flank, where the famous Lost City hydrothermal site is located (Kelley et al., 2001), is dominated by serpentinites (>70%; Karson et al., 2006). This suggests that different parts of OCCs present and record various thermal and magmatic regimes. If we focus on the area where the serpentinites are exhumed at the seafloor, the following conclusions arise.

The first 100 m beneath the seafloor correspond to a detachment shear zone, fully serpentinized, showing a strong mesoscopic foliation. The intensity of the fabric increases upwards as observed along all other detachment shear zones worldwide, including in the OCT environment (e.g. Picazo et al., 2013). Above the detachment zone, a 1–3 m thick serpentinite breccia unit has been mapped locally (Karson et al., 2006). Below the detachment shear zone, the ultramafic rocks are variably serpentinized (10 up to 80%; Fig. 7). Preserved peridotites and gabbros show a high temperature foliation, mantellic and granulitic to amphibolitic, respectively (Mével, 2003).

Within the detachment shear zone, rocks are made of discontinuous lenticular bands of dark serpentinite and lighter coloured schistose bands made of talc and Ca-amphibole showing crystal-plastic deformation (Escartín et al., 2003; Karson et al., 2006). In the partly serpentinized ultramafic rocks, serpentinite textures are locally overgrown by a talc–amphibole–chlorite assemblage, which is in turn cut by later serpentinite and/or calcite veins (Andreani et al., 2007; Boschi et al., 2006). The presence of secondary minerals such as talc, chlorite and amphibole in the foliated serpentinites results from the metasomatic circulation of Si–Ca–Al-rich fluids channelized along the foliation plane and fractures during the activity of the detachment fault (Boschi et al., 2006).

Steeply dipping shear zones with anastomosing fabric cut across the detachment shear zone and the serpentinized basement rocks, to a minimum depth of 500 m below the surface (Karson et al., 2006). These shear zones are typically 10 to 3 cm large, dipping in several directions and systematically showing normal slip displacement. The orientations and kinematic indicators of the ductile shear zones suggest that they accommodated a dominant coaxial strain with a general flattening at the top of the OCCs. Normal faults, with scarps locally higher than 500 m (Fig. 7), are the latest deformation event that also led to the brecciation of the serpentinites infilled by a stockwork of carbonate veins similar to ophicalcites 2 observed in ophiolites (see § 3.1 above; Fig. 7).

Andreani et al. (2007) thoroughly described, at 23°N along the MAR, the successive episodes of serpentinization occurring within the detachment shear zone. They show that the onset of serpentinization (V1 and V2 veins) occurred in a closed system with a low water/rock ratio. Locally, antigorite associated with brucite is also observed (Beard et al., 2009; Roumejeon and Cannat, 2014). An extensive microstructural study of a set of 278 abyssal serpentinized peridotites from the Mid-Atlantic and Southwest Indian Ridges (Roumejeon and Cannat, 2014) shows that serpentinization initiated along two intersecting sets of microfractures. The resulting microfracture network has a typical spacing of ~60 μm but most serpentinization occurs next to a subset of these microfractures that define mesh cells 100–400 μm in size. Apparent mesh rim thickness is on average 33 ± 19 μm corresponding to serpentinization extents of 70–80%. Malvoisin et al. (2012) experimentally show that mesh rims formation could be completed in a few years time.

The second episode of serpentinization corresponds to the development of the main schistosity parallel to the foliation of the former peridotite. These veins are either infilled with chrysotile or lizardite (Andreani et al., 2007; Beard et al., 2009). The third generation of veins developed during discrete incremental openings, through a local transfer of fluids (Andreani et al., 2007). The last generation of veins, V4, corresponds to an open system with high fluid-rock ratio and occurred after 50% of serpentinization. According to mineral assemblages and oxygen stable isotopy, it has been proposed that the onset of serpentinisation occurred at a temperature of about 350 °C at a minimum depth of 3–4 km beneath the seafloor (Andreani et al., 2007; Hebert et al., 1990), that is near the seismic Moho (Canales et al., 2000). One cannot exclude that the onset of serpentinisation along cracks can occur deeper, near 8 km beneath the seafloor, which corresponds to the maximum depth of reported low seismic velocities along the MAR (<8 km/s; Toomey et al., 1988; Tilmann et al., 2004). Hansen et al. (2013) recently described a 450 metre thick high-temperature mylonitic zone within the gabbros of the Kane OCC, which they interpreted as the precursor of the low temperature detachment zone and as having initiated at depths of ~7 km.

3.3. Serpentinites in subduction zone

Due to their large P–T stability field, serpentinites are potentially stable from trenches down to 120–150 km deep along the plate interface, especially for cold geothermal gradients (Fig. 2). Although direct evidence of the occurrence of serpentinites in active subduction zone is scarce, geophysical and geological evidences exist all around the Pacific. The intimate association of high pressure to ultra-high pressure (HP–UHP) metamorphic rocks with serpentinites within suture zones worldwide indeed suggests the presence of serpentinites in paleo-subduction zones (Deschamps et al., 2011, 2013; Guillot et al., 2009). We first review the field and geophysical evidence then focus on the role of serpentinites in subduction dynamics.

So far only three occurrences of serpentinites in active subduction zones have been recognized worldwide. Serpentinite clasts were recovered from drill holes in the forearc region of the Mariana Trough, on the flank of conical seamounts (Fryer et al., 1992). Their structural position and association with blueschist clasts suggest that they are derived from the shallow mantle wedge (Fryer et al., 2006). The second occurrence was discovered further northward along the same subduction system, along the Izu-Bonin forearc region (Kamimura et al., 2002). A third occurrence was found in mantle xenoliths from the Miocene Navajo Volcanic field at Four Corners (Colorado Plateau, SW USA; Smith, 2010). They consist of inclusions of antigorite peridotite, chlorite bearing harzburgite and Cr-magnetite dunite (deriving from brucite-bearing serpentinite). At the regional scale, those xenoliths are associated with fragments of Cretaceous coesite-bearing eclogite

(Helmstaedt and Sculze, 1988; Usui et al., 2003) suggesting that serpentinized peridotites and associated metamorphic rocks crystallized at a depth of about 75 km for a temperature range comprised between 500 and 750 °C (Fig. 8a).

In contrast, geophysical evidence of the presence of serpentinites is inferred to be widespread all along the Pacific subduction system (e.g., Reynard, 2013; Van Keken et al., 2011). Serpentinites are principally identified by the combination of reduced wave velocities in the

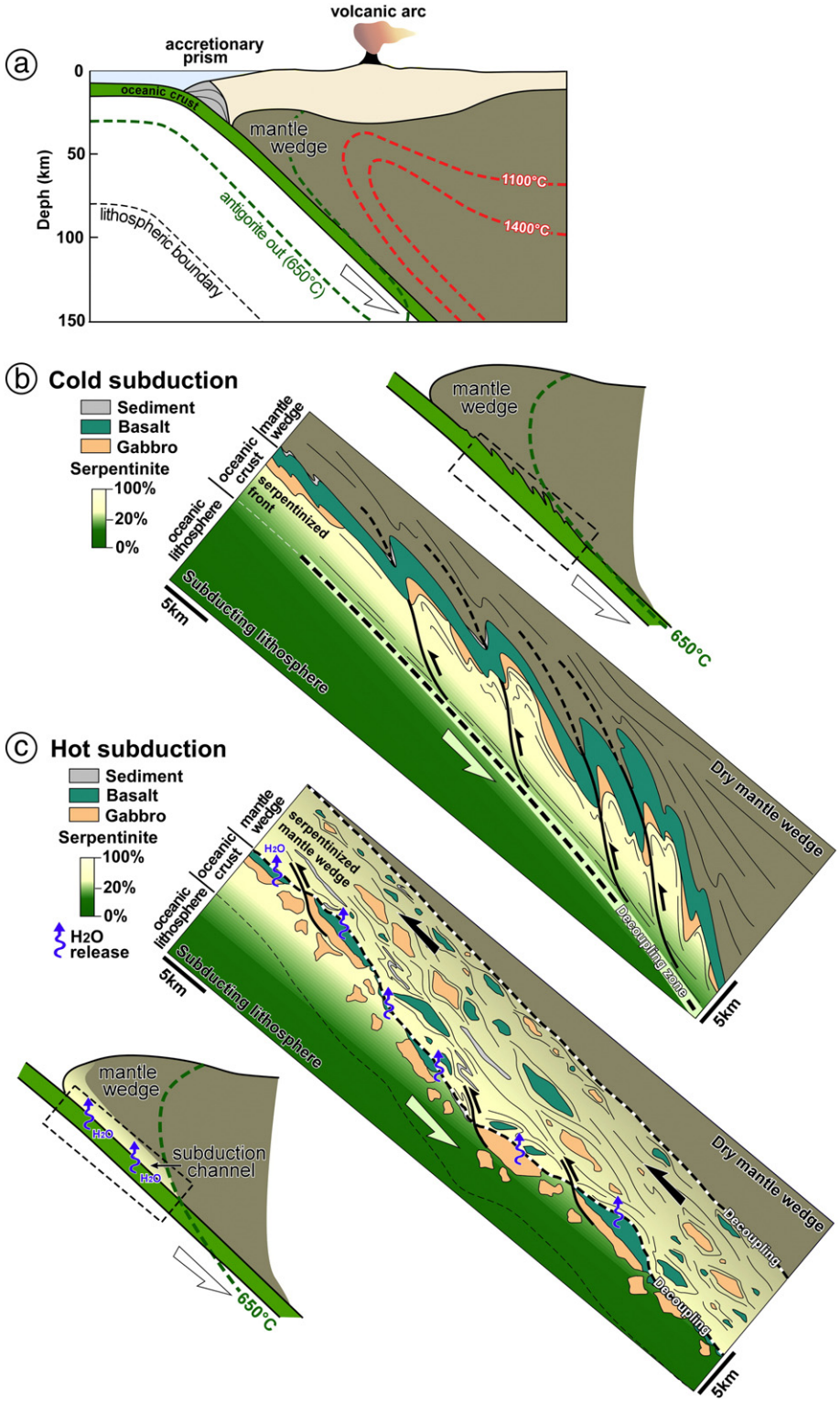

Fig. 8. Schematic sketch illustrating the geological contexts during subduction-related serpentinization; adapted from Guillot et al. (2009) and Angiboust et al. (2013b). a) General sketch an idealized subduction zone showing the relationships between the accretionnary wedge, the oceanic subduction slab and the mantle wedge. The dashed green line corresponds to the antigorite breakdown at 650 °C. b) Zoom on the subduction interface in cold subduction zone. In that case, the serpentinized front is mostly localized in the subducting plate enhancing formation of large slices of continuous "ophiolite" that can be potentially exhumed. c) Zoom on the subduction interface in hot subduction zone. In that case, both the lower and upper plates are serpentinized by fluid release upwards. This favoured the formation of tectonic mélange including serpentinites, metagabbros, metabasalts and metasediments.

mantle (Vp < 8 km/s, V_S < 4 km/s), sometimes associated with an increase of the Vp/Vs ratio to 1.8–1.85 at 10–20 km depth. The occurrence of serpentinite mud volcanoes above the low wave velocity mantle (Fryer et al., 2006; Kamimura et al., 2002; Tibi et al., 2008) is in agreement with the mantle wedge serpentinization at shallow depths. Between 30 and 80 km deep, the amount of serpentinization of the mantle wedge likely increases due to the cumulative release of fluids along warmer portions of the subducting slab (Hyndman and Peacock, 2003; Rupke et al., 2004; van Keken et al., 2011). For hot subductions this highly serpentinized zone is shifted upwards, as reflected by seismic imaging (Bostock et al., 2002). Reynard (2013) and Bezacier et al. (2013) estimated serpentinization values as high as 30–100%. In the cold mantle wedge such as Hokkaido, seismic observations show that only the plate interface is serpentinized (Nakajima et al., 2009) while in hotter subduction zones such as Costa Rica (DeShon and Schwartz, 2004), Chile (Dorbath et al., 2008) or Cascadia (Bostock et al., 2002; Ramachandran and Hyndman, 2012), the serpentinization rate is high (from 25 to 100%). In Cascadia and Mexico, geophysical data suggests that a 2–3 km thick layer could be fully serpentinized and strongly foliated (Bezacier et al., 2010a; Nikulin et al., 2009; Song et al., 2009), thus forming a thick serpentinite layer in the upper part of the plate interface (Guillot et al., 2001; or subduction channel, Shreve and Cloos, 1986). Deeper down, between 80 and 120 km, Kawakatsu and Watada (2007) described beneath NE Japan a low velocity zone above the subduction slab which they interpreted as a 1 to 10 km thick serpentinite layer. As noticed by Reynard (2013), such low-velocity zones could also be interpreted as talc- or chlorite-bearing ultramafic rocks, which have geophysical properties similar to those of serpentinites. In fact, as we will describe it later, exhumed HP to UHP serpentinites are commonly associated with chlorite and talc minerals. Serpentinization has been documented below the oceanic Moho of the subducting slab, near the trench, in Central America (Lefeldt et al., 2009; Ranero et al., 2003) and Chile (Ranero and Sallares, 2004; Contreras-Reyes et al., 2008; Lefeldt et al., 2012). This serpentinization of the slab mantle is attributed to hydrothermal circulation associated with bending and normal faulting at the outer-rise, just off the trench (Ranero et al., 2003). The penetration depth of fluids within the mantle varies from 1–2 km (Ranero et al., 2003) down to 5 km (Contreras-Reyes et al., 2008; Lefeldt et al., 2012). Whatever the uncertainties on the maximum downward extent of slab serpentinization beneath the Moho, serpentinization probably does not reach deep enough to correspond to the double Wadati–Benioff zone (unlike suggested by Faccenda et al., 2009) since seismic anisotropies are consistent with the presence of an anhydrous and deformed mantle (Reynard et al., 2010). The double Wadati–Benioff zone would thus rather relate to periodic instabilities in deforming peridotites (Kelemen and Hirth, 2007) than to serpentines and dehydration embrittlement as proposed by Peacock (2001), and Yamasaki and Seno (2003).

Serpentinites associated with HP to UHP rocks in suture zones worldwide are generally regarded as fragments of oceanic lithosphere pulled down within subduction zones (Fig. 8a; Coleman, 1971) and later exhumed by a combination of return flow and buoyancy forces (Agard et al., 2009; Gerya et al., 2002; Gorczyk et al., 2007; Guillot et al., 2009; Schwartz et al., 2001). The initial geometry is difficult to reconstruct because the original contacts (and in particular the position of the rocks with respect to either the upper or lower plate) are rarely preserved in exhumed rocks. Nevertheless, in several well-studied locations, the observed geometry has been shown to be strongly dependent on the origin of the serpentinites. Deschamps et al. (2012, 2013) indeed point out that the serpentinites associated with HP to UHP rocks can be either derived from the ocean (abyssal or oceanic continental transition) or from the mantle wedge.

In the western Alps, most of the serpentinites associated with HP–UHP rocks (Zermatt–Saas, Monviso, Lanzo) derive from an embryonic ocean or from the oceanic continental transition. They have been therefore either interpreted as a complete ophiolite sequence in which the initial oceanic contacts are relatively well preserved (Angiboust et al., 2009, 2012; Lagabrielle and Cannat, 1990; Li et al., 2004; Lombardo et al., 1978) or as a tectonic melange (Schwartz et al., 2000). The global size of those massifs is of about 30 to 60 km long for thicknesses comprised between 1 and 5 km. In these massifs, the serpentinites are strongly sheared (Fig. 3d) and dominated by the HP antigorite serpentine (Auzende et al., 2006), confirming that both serpentinites and metamafic rocks underwent similar eclogitic conditions (≈25 kbar, 550 °C). The Lanzo massif is not fully serpentinized and the oceanic front of serpentinization is well preserved (Bodinier and Godard, 2014; Debret et al., 2013). Recent investigations on Zermatt–Saas and Corsican ophiolites also demonstrated the preservation of inherited ocean–continent transitions, suggesting restricted or localized tectonic mixing during exhumation and nappe-stacking (Angiboust and Agard, 2010; Beltrando et al., 2014). The apparent tectonic complexity observed today in the field is thus attributed to large-scale boudinage (Fig. 8b) resulting from deformation of material having significant rheological contrasts (e.g., mafic rocks versus serpentinite), the existence of initial crustal heterogeneities and additional fracturing and folding during exhumation.

In contrast, HP serpentinites deriving from the mantle wedge (Deschamps et al., 2013) such as in Cuba, Dominican Republic, Guatemala or in Sistan (Eastern Iran) are systematically associated with metamorphic blocks of different sizes (from centimetre to hectometre), having different origins (tholeitic or arc basalts, OIB, metasediments), recording contrasted P–T conditions and dispersed in a strongly sheared serpentinite matrix (Fig. 8c). These observations suggest that they represent true tectonic mélanges developed along the subduction interface (Angiboust et al., 2013a; Auzende et al., 2002; Blanco-Quintero et al., 2011; Harlow et al., 2004; Krebs et al., 2011; Saumur et al., 2010).

The Voltri massif in the southwestern Alp shows intermediate features between a tectonic mélange and a preserved HP ophiolite. This massif is indeed classically considered as a slice of the OCT exposed at the seafloor during the opening of the Tethyan ocean (Piccardo and Vissers, 2007) later subducted at a depth of about 80 km with secondary olivine resulting from antigorite dehydration (Scambelluri et al., 1995). Yet B, O,–H and Sr isotope systems indicate that serpentinization of this ophiolite partly occurred within the subduction zone by fluid circulation at the plate interface giving a mantle wedge origin for the serpentinization (Scambelluri and Tonarini, 2012). In this massif, peridotite bodies show a variable degree of serpentinization. Well-preserved peridotites are surrounded by strongly foliated serpentinites and a gradual transition between them occurs (Malatesta et al., 2012). Several generations of serpentinites developed during syn-tectonic subduction, down to antigorite breakdown, and then during exhumation under greenschist facies conditions (Hermann et al., 2000; Scambelluri et al., 1995). The serpentinites are characterized by a mineralogical association of antigorite, chlorite, opaque minerals (Fe–Ni sulphide and iron oxides) and relict bastitic pyroxenes. Iron oxide levels underline the structures where deformation is pervasive (Malatesta et al., 2012). From field observations of highly sheared serpentinites wrapping mafic and ultramafic bodies and metasediments, the various metamorphic conditions in different blocks and various timing of exhumation, several authors (Federico et al., 2007; Festa et al., 2010; Malatesta et al., 2012) concluded that the Voltri massif represents a tectonic mélange developed at depth along the subduction interface (Fig. 8c).

HP serpentinites can also be associated with UHP continental units. In the Himalaya, highly sheared serpentinites wrap the Tso Morari massif and show syn-exhumation shear criteria (de Sigoyer et al., 2004; Guillot et al., 2000). While serpentinites only form a thin unit (<100 metres thick) at the hanging wall of the shear zone, the footwall corresponds to a thicker, two kilometre wide shear zone around the UHP continental unit (de Sigoyer et al., 2004). These serpentinites have a mantle wedge origin and are dominated by antigorite mineral plus secondary spinifex-like olivine, symptomatic of antigorite breakdown (Guillot et al., 2001).

3.4. Serpentinites in continental strike-slip faults

Large-scale active fault zones are characterized by slip rates of several cm/year along hundreds of kilometres and have widths of a few hundred metres. They are deeply rooted in the crust and potentially within the mantle (Teyssier and Tikoff, 1998). They are acting as plate boundaries in North America (e.g. Wallace, 1990), in Tibet (Tapponnier et al., 1982) or in Turkey (Sengör et al., 2005). The distribution of seismic activity along large-scale active strike-slip faults such as the San Andreas Fault in California (Fig. 1), the Anatolia Fault in Turkey or the Septentrional Fault Zone in Northern Caribbean reveals a partitioning between seismic, blocked and creeping segments (Manaker et al., 2008; Moore and Rymer, 2007). Weak fault behaviour characterized by low interplate coupling can be caused by high fluid pressures, high geothermal gradients or weak materials such as serpentinite and/or talc (Hirth and Guillot, 2013; Moore and Rymer, 2007). Along active fault zones, serpentinite bodies are commonly interpreted as earlier suture zones reactivated and parallelised along the fault zone (Coleman, 1971). Tectonic and geophysical investigations in California show, however, that the serpentinites outcropping along the San Andreas Fault correspond to kilometric serpentinite bodies diapirically exhumed along the fault zone (Fig. 9; Coleman et al., 2000; Kirby et al., 2014). These serpentinite bodies appear deeply connected (at depths of ~20 km) with the Franciscan mélange and the Great Valley sequence (Fig. 9). Locally, kilometric-scale serpentinite bodies crop out along the San Andreas Fault. The most famous is the 10 * 5 km New Idria massif, which is dominated by antigorite serpentinites associated with high-grade tectonic blocks of jadeite bearing eclogites and other metamorphic rocks (Tsujimori et al., 2007). The presence of eclogite blocks suggests that the New Idria serpentinite diapir was initiated at mantle depths. The wide range of P–T conditions of tectonic blocks supports the idea that the New Idria serpentinite diapir and enclosed tectonic blocks from the Franciscan complex at various mantle-crustal levels during diapiric upwelling and extrusion. Similarly, hectometre to kilometre-scale serpentinite bodies were emplaced diapirically along the active Septentrional fault zone in Hispaniola (Lewis et al., 2006). Saumur et al. (2010) showed that serpentinites along the fault zone are associated with retrogressed eclogites and have a mantle wedge signature. The presence of lizardite indicates that they in fact come from the shallower part of the mantle wedge. These serpentinites are not foliated but enclose strongly sheared amphibolitic gneisses, suggesting that they were vertically emplaced during the activity of the fault (Saumur et al., 2010). The latter authors proposed, as for serpentinites observed along the San Andreas Fault, that they protruded from the mantle wedge to the surface along the fault zone.

The recent petrological study of a diapiric serpentinite body near Redwood City (20 km south of San Francisco, California) locally bounded by a strand of the San Andreas Fault system, shows at least two major stages of serpentinization. The first one, dominated by antigorite plus brucite, occurred as in situ mantle serpentinization and was followed by a lower-temperature serpentinization with lizardite, chrysotile, and magnetite under intense deformation during the ascent of the serpentinite diapir (Kirby and Uno, 2013). North of the Parkfield segment, the 175 km long San Andrea Fault segment creeps at a rate of 28 mm/year. Over the last 40 years, hundreds of earthquake events smaller than Mw4, and about 50 earthquake events smaller than Mw6, occurred in Northern California (Earthquake Data Center, NCEDC), the most recent being the 2004 Mw6 Parkfield earthquake. It was proposed that, in this region, serpentinites deriving from the Great Valley Formation have been associated with fault creep (e.g., Moore and Rymer, 2007). The SAFOD project (San Andreas Fault Observatory at Depth) drilled and instrumented the SAF just north of Parkfield city (Fig. 9). Microstructural observations from core samples show evidence of deformation within the 200 metre thick damaged zone (Gratier et al., 2011). Moore and Rymer (2007) also reported talc from cuttings. Moore and Rymer (2011) show that, at 3 km depth, the creeping area mainly consists of clasts of serpentinites and sedimentary rocks dispersed in a matrix of saponite, a trioctahedral Mg-rich smectite clay ($Ca_{0.25}(Mg,Fe)_3((Si,Al)_4O_{10})(OH)_2 \cdot n(H_2O)$). Saponite is a very weak mineral (frictional strength <0.10) deriving from the alteration of serpentine in the presence of quartzofeldspathic rocks at temperatures <150 °C, which can explain the average low frictional strength of about 0.15 in the first 3 km of the creeping zone.

4. Discussion

According to the description of regional examples presented in the previous section, we will refocus in this section on the role of serpentinites in general tectonic processes.

4.1. Role of serpentinites at the OCT

The three main features of rifting at magma poor-margin are (1) an almost 100 km wide hyperextended crust, (2) the absence of the lower continental crust and (3) the serpentinized continental mantle exhumed at the sea floor. According to onshore and offshore observations (e.g. Mohn et al., 2012; Picazo et al., 2013; Sutra et al., 2013), rifting evolution can be divided into three main phases. During the first phase, crustal thinning is accommodated by conjugate crustal-scale shear

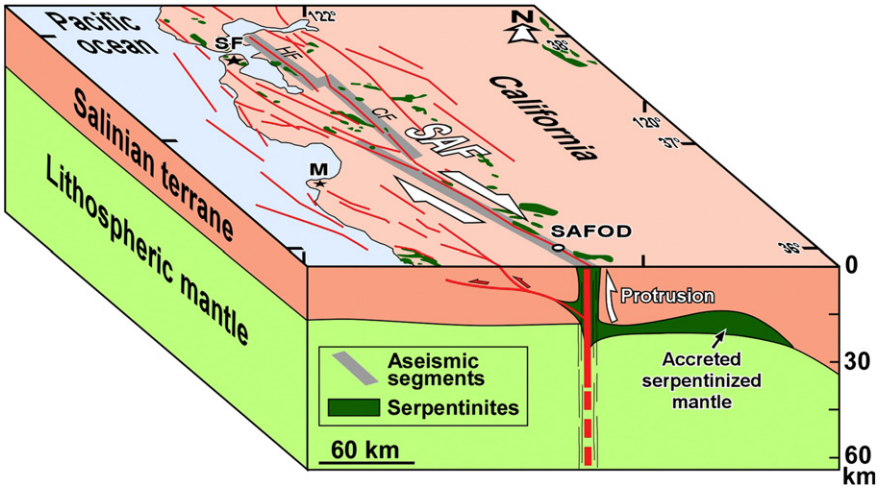

Fig. 9. Schematic 3-D block diagram of distribution of serpentinite outcrops in central California and localization of major faults with creeping (aseismic) segments (modified after Hirth and Guillot, 2013; Kirby et al., 2014). Mantle wedge related serpentinites protruded along the majors strands of the Sand Andreas Fault, lubricating the creeping segments. SF, San Francisco; M, Monterey; SAF, San Andreas Fault; HF, Hayward Fault; CF, Calaveras Fault, SAFOD, San Andreas Fault Observatory at Depth.

zones and by ductile flow of the middle crust (Fig. 6). At this stage, the lower part of the continental mantle moves upward along the top to the continental localized shear zones (Huismans and Beaumont, 2012). It allows the lower part of the upper mantle to be progressively exhumed and impregnated by mafic magmas, leading to the crystallization of pyroxenite dykes parallel to the main foliation (Le Roux et al., 2007). Locally, HT amphiboles crystallize from silica-rich fluids. At this stage, it is difficult to decipher the origin of the fluids. It can be either released during crystallization of the MOR magmas (deep fluids), as the mantle contains up to 500 ppm of water in the pyroxene (Bell and Rossman, 1992), or coming from the dehydration of the continental crust (shallow fluids). The combination of increasing strain in the mantle and the onset of fluid circulation at medium temperature (1000–800 °C) favoured at this stage the localization of deformation in a mylonitic shear zone as observed in the Totalp unit (Picazo et al., 2013). The mylonite is located within grain size/stress domain where dislocation-accommodated grain boundary sliding (disGBS) creep is activated, a deformation mechanism that strongly reduces the mantle strength (Précigout and Gueydan, 2009). According to Gueydan and Précigout (2014), this weakening of the mantle provokes its coupling with the ductile lower/intermediate continental crust, triggering the hyperextension of the whole crust (thickness >10 km) at the onset of rifting.

The second stage of rifting is characterized by the penetration of seawater along high-angle brittle normal faults down to the mantle (Fig. 6). At this stage the top of the mantle is sufficiently cooled (<800 °C) to first crystallize Mg-Hornblende rich peridotites and chlorite-rich peridotites and is then rapidly and pervasively serpentinized. The peak of serpentinization occurs at a temperature of about 300–350 °C. The serpentinization of the upper mantle strongly modifies its rheology, making it too weak to remain coupled with the crust. Consequently, the ongoing extension allows the top serpentinized mantle to be exhumed oceanward relative to the continental crust along a low angle hectometre thick detachment fault (S-reflexion of Reston et al., 1996). The very rapid exhumation of the serpentinized mantle, up to 3 cm/year for the mantle at the Iberia margin (Sutra et al., 2013), allows the strain to be accommodated by both brittle (cataclasite) and ductile (gouge) deformations. Fluid interactions with local gabbroic bodies and/or first deposited sediments lead to the formation of the rheologically weak talc within serpentinized shear zones (Escartín et al., 2008).

The final stage occurs at the seafloor with penetration of alkaline fluids along the fault system leading to carbonatation of the serpentinite. Stable isotopes suggest that this late event occurs at a temperature of about 100 °C (Früh-Green et al., 1990; Skelton and Valley, 2000). Dismantling of serpentinite escarpments produced by high angle normal faults provokes the formation of debris-flow (ophicalcite 2; Lemoine et al., 1987).

4.2. Role of serpentinites at slow to ultra-slow spreading ridges

The role of serpentinite is crucial for the development of long-term detachment faulting in oceanic domains. It has been proposed that the initiation of the detachment fault occurred by the downward propagation of steep normal faults from the seafloor to the weak mantle hydrated by magmatic fluids and surrounding gabbro plutons emplaced at a depth of about 7–8 km (Ildefonse et al., 2007; Nozaka and Fryer, 2011). At this stage, serpentinization is probably not effective as the temperature is too high (>700 °C), but mantle strain localization mechanisms enable the lithospheric-scale detachment fault to form (Blackman et al., 2011). The progressive exhumation of the hanging wall leads to the cooling of the detachment shear zone and to associated, progressive seawater infiltration allowing the mantle serpentinization and the lubrication of the localized shear zone. Another major effect of the serpentinization is to reduce the strength of the lithosphere, thereby facilitating the bending of the detachment fault and its roll-over (Fig. 7). Cannat et al. (2009) and Sauter et al. (2013) proposed that the final geometry of the exhumed mantle is directly correlated with the proportion of gabbros relative to the serpentinites. At high serpentinite/gabbro ratio (>90/10), the detachment footwall had a larger rigidity than during the formation of a corrugated surface, where the serpentinite/gabbro ratio is <10/90. In the former case, the detachment displays a large curvature, corresponding to a large and flat detachment fault with important displacement (>17 km) and a relatively smooth and low relief (≈500 m) relative to the axial domain. This flat-lying detachment fault is also crosscut by several high angle normal faults that have been possibly reactivated when the new detachment fault dips on the opposite side (Sauter et al., 2013). At low serpentinite/gabbro ratio, serpentinites are strongly altered and produce secondary minerals (talc and chlorite essentially) that are even mechanically weaker (Escartín et al., 2008; Morrow et al., 2000). Bending curvature is lower and OCC consequently develops over a shorter distance (<10 km wide) and with a higher associated relief (>3000 m). The deformation is localized in the first 100 metre thick upper detachment shear zone made of very weak metasomatised serpentinites wrapping the gabbroic crust (Blackman et al., 2011). The rheological contrast between the rigid cooled gabbroic bodies and the very weak serpentinized layer allows the displacement of the footwall to be localized in this 100 metre thick zone (Ildefonse et al., 2007).

4.3. Role of serpentinite in subduction zones

In order to be consistent with surface heat flow measurements in subduction zones (for a discussion of the geophysical signature of serpentinite and serpentinization in subduction zone, see Reynard, 2013), current mantle wedge corner flow models require decoupling between the subducting slab and the overlying mantle wedge (e.g., Syracuse et al., 2010; Wada et al., 2008 and references therein). This decoupling results in a stagnant wedge corner, which in turn accounts for the low heat flux anomaly observed between the trench and the arc. The hypothesis that better explains this tectonic decoupling between the stagnant mantle wedge and the subducting plate is the occurrence of a weak layer of serpentinites, of a minimum thickness of 100 m, having a viscosity on the order of 10^{17} to 10^{18} Pa·s (Wada et al., 2008). Such a decoupling serpentinized zone plays a major role in the exhumation of HP to UHP rocks (Blanco-Quintero et al., 2011; Guillot et al., 2001, 2009; Hilairet and Reynard, 2009; Hilairet et al., 2007; Schwartz et al., 2001).

Global seismic tomography reveals a pronounced geometrical, thermal and kinematical asymmetry between the two plates of a subduction zone (King, 2001; Syracuse et al., 2010; Zhao, 2004). Subduction processes are often studied numerically or analogically with the use of initial asymmetric models while in global mantle convection models, where this asymmetry is not prescribed, subduction is symmetrical involving subduction of the two plates (Tackley, 2000). Thus, it is now commonly admitted that one-sided subduction requires a low strength interface between the two plates. Gerya et al. (2008) and Crameri et al. (2012) numerically explored initiation of subduction and concluded that one-sided subduction is caused by the localization of deformation in a shallow and weak hydrated shear zone. Serpentinite is thus a good candidate accounting for this weak shear zone. This serpentinite layer cannot be explained by the early hydration of the mantle wedge, however, and must predate the initiation of subduction. As discussed in § 3.1, Atlantic-type continental margins are highly serpentinized even at the sea floor. The “S-reflector” dipping beneath the continent and interpreted as the contact between the hyperextended crust and the serpentinized mantle (Reston et al., 1996; Sutra and Manatschal, 2012) is therefore a good candidate to initiate one-sided subductions at continental margins. Subduction and exhumation of the OCT all along the Alpine realm (Beltrando et al., 2014) strengthen this hypothesis. The initiation of one-sided intra-oceanic subduction could also be driven by the occurrence of serpentinites at or close to the seafloor. As discussed in Section 3.2,

slow to ultra-slow spreading oceanic environment are indeed characterized by asymmetric master normal faults coated by serpentinites that could help localizing the deformation in a later compressive context, as suggested by Ulrich et al. (2010) for the New-Caledonia ophiolite.

The role of serpentinite acting as a lubricant for the exhumation of HP to UHP rocks is a relatively recent concept proposed by Guillot et al. (2000) and Hermann et al. (2000), following earlier observations by Hoogerdjuin-Strating and Vissers (1991) in the Himalaya and in the Alps. Those models largely expand on the seminal paper of Cloos (1982) proposing that a soft matrix (in that case sedimentary) allows for the exhumation of HP blocks accordingly to a return flow parallel to the descent flow. The first numerical models by Schwartz et al. (2001) and Gerya et al. (2002) effectively show that a soft matrix having a viscosity as low as the viscosity of serpentinite can control the exhumation of kilometric eclogitic blocks from depths of about 70–80 km. This depth range coincides with the nominal depths reached by most of the exhumed oceanic eclogites worldwide and with the onset of antigorite breakdown in most of the subduction zones (Agard et al., 2009; Guillot et al., 2009). Those initial models have been refined taking into account two forces contributing to the exhumation of HP to UHP rocks: the boundary forces related to the subduction zone itself and the internal forces induced by the density difference between the subducting slab and the surrounding rocks. Both hydrated mafic rocks and serpentinites for the slab indeed reduce the average density of the whole exhumed eclogitic unit (Agard et al., 2009; Angiboust and Agard, 2010; Guillot et al., 2009; Hacker et al., 2013; Hilairet and Reynard, 2009).

None of these models, however, explain the existence of the two different types of eclogitic massifs exhumed worldwide: well preserved HP ophiolitic massifs and HP tectonic mélanges, sometimes in close association (Angiboust et al., 2013a). One possibility is that the preservation of a HP complete oceanic sequence or the formation of HP tectonic mélange reflects the initial geometry (as recalled in § 3.2 slow-spreading oceanic lithosphere can be initially highly heterogeneous) and/or the thermal regime of oceanic lithosphere prior to subduction. In a recent model, Angiboust et al. (2013b) proposed an explanation highlighting the role of serpentinites in the final geometry of the HP exhumed unit. They show that if the oceanic mantle beneath the normal oceanic crust is serpentinized before entering the subduction zone (see Section 3.3.1), this creates a kilometric thick, buoyant and weak layer enhancing the basal decoupling responsible for the detachment of continuous slices at depth (Fig. 8). Their experiments show that large, plural-kilometric volumes of oceanic lithosphere can be accreted between 50 and 110 km along the subduction interface. Angiboust et al. (2013b) also suggest that the reversed polarity of km-size HP ophiolitic units, such as the Monviso unit, may in part result from kilometre-scale drag folds formed during the exhumation (Fig. 8), due to the viscosity contrast between the relatively rigid blocks of metagabbro–metabasalt and the soft serpentinite (such as in alternations of limestone and clay or migmatites; Ramsay and Huber, 1987).

Interestingly, Angiboust et al. (2013b) also show that when the subduction interface is soft enough (due to the occurrence of extensive metasediments, or to a layer of serpentinites and/or hydrated basalt), this causes the partial hydration of the mantle wedge and the development of a tectonic mélange, i.e., a soft matrix deriving from the upper and the lower plates (Fig. 8c). An indirect consequence of this model is that we can predict that tectonic mélanges preferentially develop in warm subduction zone because, in this context, the hydration of the mantle wedge by fluid release from the subducting plate is favoured (e.g., Peacock and Wang, 1999; Syracuse et al., 2010). For example, serpentinite tectonic mélanges are often associated with magmatic arc development, as in Guatemala, Cuba and in the Dominican Republic, advocating for past warm subductions (e.g., García-Casco et al., 2006; Guillot et al., 2009 and references therein).

We thus propose the following explanation to reconcile the two types of HP units observed worldwide (Fig. 8):

(1) Continuous HP ophiolite slices would form in cases of initial oceanic settings not too strongly altered (and thereby not too rheologically weakened) before subduction, and mostly metastably preserved and exhumed at the end of oceanic subduction as a result of the entrance of a buoyant continent (Angiboust and Agard, 2010). Their exhumation is only possible if the oceanic mantle is partly serpentinized, allowing for the decoupling with the ongoing subducted slab.
(2) In contrast, HP tectonic mélanges would derive from strongly altered (i.e., where serpentinites are already at the seafloor; amagmatic center, Cannat, 1993) and/or warm (or young) initial oceanic settings promoting the transfer of fluids from the upper part of the slab to the mantle wedge and significant mixing along the interface.

4.4. Role of serpentinites in continental strike-slip faults

The distribution of seismic activity along San Andreas active faults, and also along the Septentrional fault in the Northern Caribbean or the North Anatolian fault in Turkey, reveals a partitioning between seismic and creeping segments (Karabacak et al., 2011; Saumur et al., 2010; Schulz et al., 1982). Serpentinites formed by the hydration of mantle peridotites are present at several locations along these faults and are particularly common along the creeping segment of the San Andreas Fault system (Fig. 9) north of Parkfield (Kirby et al., 2014; Moore and Rymer, 2007), along the seismic gap in the Rio San Juan area in the Dominican Republic (Calais et al., 2010; Saumur et al., 2010) and in the central part of the North Anatolian fault, in the Ismetpasa and Destek sections (Karabacak et al., 2011). These creeping segments suggest a low interseismic plate coupling (Manaker et al., 2008) compatible with low frictional strength. As already discussed, experiments reveal that serpentinites have a relatively high frictional strength of about 0.6–0.7 at room temperature (Reinen et al., 1994), a range that is equivalent to most other silicate rocks. Experiments on wet chrysotile-dominated gouges show a positive temperature-dependence on rheology (Moore et al., 1996, 1997). The apparent tectonic softening of serpentinites inferred from field observations has thus long been an enigma and the role of water released by serpentine dehydration has been suspected as a solution to it (Faulkner and Rutter, 2001; Raleigh and Paterson, 1965). Kirby et al. (2014) proposed that deep dehydration of pressurized water in the forearc mantle, beneath the San Andreas Fault zone, could help the upward migration of blocks of forearc mantle serpentinites (Fig. 9). Their ascent would be driven in part by buoyancy, due to their low density, and by reducing the effective-normal-stress along faults bounding these serpentinized blocks or slivers. The formation of weak alteration by-products during the ascent of such serpentinite-rich fluids, such as talc, chrysotile, saponite and brucite, and also pressure-solution recrystallization in the quartzo-feldpathic rocks may also play a supplementary role in fault-zone weakening (Andreani et al., 2005; Gratier et al., 2011; Moore et al., 2004; Schleicher et al., 2010). Indirect evidence of such fluids comes from the common occurrence of different crystalline forms of serpentine (antigorite, lizardite, and chrysotile) in the same serpentinite outcrop (Kirby et al., 2014; Saumur et al., 2010), suggesting multiple stages of mineral formation over different temperature ranges.

5. Conclusion

Hess (1955) first proposed that alpine peridotites were emplaced in mountain ranges by cumulative small shear displacements on numerous faults. He compared this process of intrusion to squeezing a watermelon seed between two fingers. Raleigh and Paterson (1965) experimentally confirmed that a serpentinite, made of a mixture of lizardite, chrysotile and brucite, shows a loss of strength at

300–350 °C, while an antigorite bearing serpentinite becomes weak above 500–600 °C. He proposed that the strength reduction results from a combination of embrittlement and water release during partial dehydration. Recent experiments confirm that serpentinite acts as a lubricant (Chernak and Hirth, 2010; Hilairet et al., 2007) and therefore plays a major role in dynamic settings. Serpentinites only represent 3 to 4% of the earth's surface (Guillot and Hattori, 2013). Nevertheless, we show in this review paper that whatever the tectonic setting, continental rifting, slow to ultra-slow oceanic spreading, subduction and large-scale strike-slip faulting, whenever serpentinites or by-products deriving from their alteration or metamorphism are geologically or geophysically observed, they play a major role at temperatures <700 °C, from 0 to 150 km depth. When water is available, serpentinites and associated rocks weaken the strong upper mantle and are embedded in, or diapirically intrude, the continental crust. They thus allow the deformation to get localized within narrow, hundreds of metres thick shear zones, accommodating kilometres of vertical or horizontal displacements at a rate of cm/year. In the deep lithosphere, the accumulation of damage in olivine triggers shear (Bercovici and Ricard, 2014) while, in the upper lithosphere, the presence of serpentinites is key to ensure long-lived weak zones at plate boundaries, and more generally plate tectonics. Due to the importance of phyllosilicates and especially serpentine minerals in plate tectonic processes, further experimental improvements are necessary including mechanism of syntectonic crystal growth, dynamic of fluid transfer during hydration and dehydration processes, and finally establishing reliable physical laws for extrapolation.

Acknowledgements

This article benefits from helpful discussions during the last ten years with M. Andreani, S. Angiboust, A.L. Auzende, A. Baronnet, F. Boudier, A.M. Boullier, M. Cannat, B. Debret, B. Devouard, J. Escartin, B. Evans, A. Garcia-Casco, T. Gerya, M. Godard, W. Gorczyk, K.H. Hattori, N. Hilairet, G. Hirth, B. Ildefonse, Y. Lagabrielle, G. Manaschal, C. Mével, O. Müntener, M. Scambelluri, M. Ulrich, and B. Wunder. The authors are grateful to Tim Horscroft for encouraging them to write this contribution. R.L. Carlson and an anonymous reviewer are warmly thanked for scientific comments and reviews. SG and PA acknowledge funding from the ANR project O:NLAP and the labex OSUG@2020. BR acknowledges funding from the Programme National de Planétologie of Institut National des Sciences de l'Univers.

References

Agard, P., Yamato, P., Jolivet, L., Burov, E., 2009. Exhumation of oceanic blueschists and eclogites in subduction zones: timing and mechanisms. Earth Sci. Rev. 92, 53–79.
Amiguet, E., Reynard, B., Caracas, R., Van de Moortèle, B., Hilairet, N., Wang, Y., 2012. Creep of phyllosilicates at the onset of plate tectonics. Earth Planet. Sci. Lett. 345–348, 142–150.
Amiguet, E., Van De Moortèle, B., Cordier, P., Hilairet, N., Reynard, B., 2014. Deformation mechanisms and rheology of serpentines in experiments and in nature. J. Geophys. Res. http://dx.doi.org/10.1002/2013JB010791.
Andreani, M., Boullier, A.M., Gratier, J.P., 2005. Development of schistosity by dissolution–crystallization in a Californian serpentinite gouge. J. Struct. Geol. 27, 2256–2267.
Andreani, M., Mevel, C., Boullier, A.-M., Escartin, J., 2007. Dynamic control on serpentine crystallization in veins: constraints on hydration processes in oceanic peridotites. Geochemistry Geophysics Geosystems 8, 1–24.
Andreani, M., Muñoz, M. Marcaillou C., Delacour, A., 2013. μXANES study of iron speciation in serpentine during oceanic serpentinization. Lithos 178, 70–83.
Angiboust, S., Agard, P., 2010. Initial water budget: the key to detaching large volumes of eclogitized oceanic crust along the subduction channel? Lithos 120, 453–474.
Angiboust, S., Agard, P., Jolivet, L., Beyssac, O., 2009. The Zermatt–Saas ophiolite: the largest (60-km wide) and deepest (c. 70–80 km) continuous slice of oceanic lithosphere detached from a subduction zone? Terra Nova 21, 171–180.
Angiboust, S., Langdon, R., Agard, P., Waters, D., Chopin, C., 2012. Eclogitization of the Monviso ophiolite and implications on subduction dynamics. J. Metamorph. Geol. 30, 37–61.
Angiboust, S., Agard, P., De Hoog, J.C.M., Plunder, A., 2013a. Insights on deep, accretionary subduction processes from the Sistan ophiolitic "mélange" (Eastern Iran). Lithos http://dx.doi.org/10.1016/j.lithos.2012.11.007.
Angiboust, S., Wolf, S., Burov, E., Agard, P., Yamato, P., 2013b. Effect of fluid circulation on subduction interface tectonic processes: insights from thermo-mechanical numerical modelling. Earth Planet. Sci. Lett. 358, 238–248.
Aumento, F., Loubat, H., 1971. The Mid-Atlantic Ridge near 45°N. Serpentinized ultramafic intrusions. Can. J. Earth Sci. 8, 631–663.
Auzende, A.-L., Devouard, B., Guillot, S., Daniel, I., Baronnet, A., Lardeaux, J.-M., 2002. Serpentinites from Central Cuba: a Petrologic, Raman and HRTEM study. Eur. J. Mineral. 14, 905–914.
Auzende, A.L., Guillot, S., Devouard, B., Baronnet, A., 2006. Serpentinites in Alpine convergent setting: effects of metamorphic grade and deformation on microstructures. Eur. J. Mineral. 18, 21–33.
Auzende, A.L., Escartin, J., Walte, N., Guillot, S., Frost, D., 2015. Deformation mechanisms of antigorite serpentinite at subduction conditions from experimentally and naturally deformed rocks. Earth Planet. Sci. Lett. 411, 229–240.
Bach, W., Garrido, C.J., Paulick, H., Harvey, J., Rosner, M., 2004. Seawater-peridotites interactions: first insights from Odp Leg 209, Mar 15°N. Geochem. Geophys. Geosyst. 5. http://dx.doi.org/10.1029/2004GC000744.
Bascou, J., Barruol, G., Vauchez, A., Mainprice, D., Egydio-Silva, M., 2001. EBSD measured lattice-preferred orientations and seismic properties of eclogites. Tectonophysics 342, 61–80.
Beard, J.S., Frost, B.R., Fryer, P., McCaig, A., Searle, R., Ildefonse, B., Zinin, P., Sharma, S.K., 2009. Onset and progression of serpentinization and magnetite formation in olivine-rich troctolite from IODP Hole U1309D. J. Petrol. 50, 387–403.
Bell, D.R., Rossman, G.R., 1992. Water in earth's mantle: the role of nominally anhydrous minerals. Science 255, 1391–1397.
Beltrando, M., Manatschal, G., Mohn, G., Dal Piaz, G.V., Vitale Brovarone, A., Masini, E., 2014. Recognizing remnants of magma-poor rifted margins in high-pressure orogenic belts: the Alpine case study. Earth-Sci. Rev. http://dx.doi.org/10.1016/j.earscirev.2014.01.001.
Bercovici, D., Ricard, Y., 2014. Plate tectonics, damage and inheritance. Nature http://dx.doi.org/10.1038/nature13072.
Bernoulli, D., Jenkyns, H.C., 1974. Alpine Mediterranean and central Atlantic Mesozoic facies in relation to the early evolution of the Tethys. In: Dott, R.H., Shaver, R.H. (Eds.), Modern and Ancient Geosynclinals Sedimentation, A Symposium: Special Publication Society Economy Paleontology Mineralogy. 19, pp. 129–160.
Beslier, M.-O., Girardeau, J., Boillot, G., 1990. Kinematics of peridotite emplacement during North Atlantic continental rifting, Galicia, NW Spain. Tectonophysics 184, 321–343.
Bezacier, L., Reynard, B., Bass, J.D., Sanchez-Valle, C., Van de Moortèle, B., 2010a. Elasticity of antigorite, seismic detection of serpentinites, and anisotropy in subduction zones. Earth Planet. Sci. Lett. 289, 198–208.
Bezacier, L., Reynard, B., Bass, J.D., Wang, J., Mainprice, D., 2010b. Elasticity of glaucophane, seismic velocities and anisotropy of the subducted oceanic crust. Tectonophysics 494, 201–210.
Bezacier, L., Reynard, B., Bass, J.D., Cardon, H., Montagnac, G., 2013. High-pressure elasticity of serpentine, and seismic properties of the hydrated mantle wedge. J. Geophys. Res. Solid Earth 118, 1–9.
Blackman, D.K., 2002. Geology of the Atlantis Massif (MAR 30°N): implications for the evolution of an ultramafic oceanic core complex, MAR. Mar. Geophys. Res. 23, 443–469.
Blackman, D.K., et al., 2011. Drilling constraints on lithospheric accretion and evolution at Atlantis Massif, Mid-Atlantic Ridge 30°N. J. Geophys. Res. 116, B07103. http://dx.doi.org/10.1029/2010JB007931.
Blanco-Quintero, I.F., Garcia-Casco, A., Gerya, T.V., 2011. Tectonic blocks in serpentinite mélange (eastern Cuba) reveal large-scale convective flow of the subduction channel. Geology 39, 79–82.
Bodinier, J.-L., Godard, M., 2014. Orogenic, ophiolitic, and abyssal peridotites. In: Holland, H.D., Turekian, K.K. (Eds.), Treatise on Geochemistry, Second Edition . 3. Elsevier, Oxford, pp. 103–167.
Bodinier, J.L., Vasseur, G., Vernieres, J., Dupuy, C.F.J., 1990. Mechanisms of mantle metasomatism: geochemical evidence from the Lherz orogenic peridotite. J. Petrol. 31, 597–628.
Boillot, G., Grimaud, S., Mauffret, A., Mougenot, D., Kornprobst, J., Mergoil-Daniel, J., Torrent, G., 1980. Ocean–continent boundary of the Iberian margin: a serpentinite diapir west of the Galicia bank. Earth Planet. Sci. Lett. 48, 23–34.
Bonatti, E., Emiliani, C., Ferrara, G., Honnorez, J., Rydell, H., 1974. Ultramafic-carbonate breccias from the equatorial Mid-Atlantic Ridge. Mar. Geol. 16 (2), 83–102.
Bonatti, E., Ottonello, G., Hamlyn, P.R., 1986. Peridotites from the Island of Zabargad (St. John), Red Sea. petrology and geochemistry. J. Geophys. Res. 91, 599–631. http://dx.doi.org/10.1029/JB091iB01p00599.
Boschi, C., Früh-Green, G.L., Escartin, J., 2006. Occurrence and significance of serpentinite-hosted, talc- and amphibole-rich fault rocks in modern oceanic settings and ophiolite complexes: an overview. Ofioliti 31, 129–140.
Bostock, M.G., Hyndman, R.D., Rondenay, S., Peacock, S.M., 2002. An inverted continental Moho and serpentinization of the forearc mantle. Nature 417, 536–538.
Bromiley, G.D., Pawley, A.R., 2003. The stability of antigorite in the systems MgO-SiO2–H2O (MSH) and MgO-Al2O3-SiO2–H2O (MASH): The effects of Al3+ substitution on high-pressure stability. American Mineralogist 88, 99–108.
Boudier, F., Baronnet, A., Mainprice, D., 2010. Serpentine mineral replacements of natural olivine and their seismic implications: oceanic lizardite versus subduction related antigorite. J. Petrol. 51, 495–512.
Burov, E., Watts, A.B., 2006. The long-term strength of continental lithosphere: "jelly sandwich" or "crème brûlée". GSA Today 16, 1–5.

Calais, E., Freed, A., Mattioli, G., Amelung, F., Jonsson, S., Jansma, P., Hong, S.H., Dixon, T., Prepetit, C., Momplaisir, R., 2010. The January 12, 2010, Mw 7.0 earthquake in Haiti: context and mechanism from an integrated geodetic study. Nat. Geosci. http://dx.doi.org/10.1038/NGEO992.

Canales, J.P., Collins, J.A., Escartin, J., Detrick, R.S., 2000. Seismic structure across the rift valley of the Mid-Atlantic Ridge at 23° 20′N (MARK area): implications for crustal accretion processes at slow-spreading ridges. J. Geophys. Res. 105 (28), 411–428 (425).

Cann, J.R., Blackman, D.K., Smith, D.K., McAllister, E., Janssen, B., Mello, S., Avgerinos, E., Pascoe, A.R., Escartín, J., 1997. Corrugated slip surfaces formed at North Atlantic Ridge-transform intersections. Nature 385, 329–332.

Cannat, M., 1993. Emplacement of mantle rocks in the sea-floor at mid-ocean ridges. J. Geophys. Res. Solid Earth 98, 4163–4172.

Cannat, M., Sauter, D., Mendel, V., Ruellan, E., Okino, K., Escartin, J., Combier, V., Baala, M., 2006. Modes of seafloor generation at a melt-poor ultra-slow-spreading ridge. Geology 34, 605–608.

Cannat, M., Sauter, D., Escartín, J., Lavier, L., Picazo, L., 2009. Oceanic corrugated surfaces and the strength of the axial lithosphere at slow spreading ridges. Earth Planet. Sci. Lett. 288, 174–183.

Cannat, M., Fontaine, F., Escartín, J., 2010. Serpentinization at slow-spreading ridges: extent and associated hydrogen and methane fluxes. In: Rona, P., et al. (Eds.), Diversity of Hydrothermal Systems on Slow Spreading Ocean Ridge. American Geophysical Union Geophysical Monograph 188, pp. 241–264.

Capitani, G., Mellini, M., 2004. The modulated crystal structure of antigorite: The m = 17 polysome. Am. Mineral. 89, 147–158.

Carlson, R.L., 2001. The abundance of ultramafic rocks in Atlantic Ocean crust. Geophys. J. Inter. 144, 37–48.

Carlson, R.L., Miller, D.J., 2003. Mantle wedge water contents estimated from seismic velocities in partially serpentinized peridotites. Geophys. Res. Lett. 30, 1250.

Carlson, R.L., Miller, D.J., 2004. Influence of pressure and mineralogy on seismic velocities in oceanic gabbros: implications for the composition and state of the lower oceanic crust. J. Geophys. Res. 109, B0925. http://dx.doi.org/10.1029/2003JB002699.

Chernak, L.J., Hirth, G., 2010. Deformation of antigorite serpentinite at high temperature and pressure. Earth Planet. Sci. Lett. 296, 23–33.

Chian, D., Louden, K., Minshull, T.A., Whitmarsh, R.B., 1999. Deep structure of the ocean–continent transition in the southern Iberia Abyssal Plain from seismic refraction profiles: Ocean Drilling Program (Legs 149 and 173) transect. J. Geophys. Res. 104, 7443–7462.

Chollet, M., Daniel, I., Koga, K.T., Morard, G., van de Moortele, B., 2011. Kinetics and mechanism of antigorite dehydration: implications for subduction zone seismicity. J. Geophys. Res. Solid Earth 116. http://dx.doi.org/10.1029/2010JB007739.

Christensen, N.I., 2004. Serpentinites, peridotites, and seismology. Int. Geol. Rev. 46, 795–816.

Clerc, C., Lagabrielle, Y., Neumaier, M., Reynaud, J.Y., de Saint Blanquat, M., 2012. Exhumation of subcontinental mantle rocks: evidence from ultramafic-bearing clastic deposits nearby the Lherz peridotite body, French Pyrenees. Bull. Soc. Geol. Fr. 183, 443–459.

Cloos, M., 1982. Flow melanges: numerical modelling and geological constraints on their origin in the Franciscan subduction complex. Geol. Soc. Am. Bull. 93, 330–345.

Coleman, R.G., 1971. Plate tectonic emplacement of upper mantle peridotites along continental edges. J. Geophys. Res. 76, 1212–1222.

Coleman, R.G., 1977. Ophiolites, Ancient Oceanic Lithosphere? Springer-Verlag, Berlin, Heidelberg, New York (229 pp.)

Coleman, R.G., 2000. Prospecting for ophiolites along the California continental margin. In: Delek, Y., Moores, E.M., Elthon, D., Nicolas, A. (Eds.), Ophiolites and Oceanic Crust: New Insights From Field Studies and the Ocean Drilling Program. Geological Society of America Special Paper 349, pp. 351–364.

Contreras-Reyes, E., Grevemeyer, I., Flueh, E.R., Reichert, C., 2008. Upper lithospheric structure of the subduction zone offshore of southern Arauco Peninsula, Chile, at similar to 38 degrees S. J. Geophys. Res. Solid Earth 113, B07303.

Crameri, F., Schmeling, H., Golabek, G.J., Duretz, T., Orendt, R., Buiter, S.J.H., May, D.A., Kaus, B.J.P., Gerya, T.V., Tackley, P.J., 2012. A comparison of numerical surface topography calculations in geodynamic modelling: an evaluation of the 'sticky air' method. Geophys. J. Inter. 189, 38–54.

de Sigoyer, J., Guillot, S., Dick, P., 2004. Exhumation processes of the high-pressure low-temperature Tso Morari dome in a convergent context (eastern-Ladakh, NW-Himalaya). Tectonics 23 (3), TC3003. http://dx.doi.org/10.1029/2002TC001492.

Debret, B., Nicollet, C., Andreani, M., Schwartz, S., Godard, M., 2013. Three steps of serpentinization in an eclogitised oceanic serpentinisation front (Lanzo massif — Western Alps). J. Metamorph. Geol. 31, 165–186.

Decandia, F.A., Elter, P., 1972. La zona ofiolitifera del Bracco nel settore compreso fra Levanto e la Val Graveglia (Appennino Ligure). Mem. Soc. Geol. Ital. 11, 503–530.

Deschamps, F., Guillot, S., Godard, M., Andréani, M., Hattori, K.H., 2011. Serpentinites act as sponges for fluid-mobile elements in abyssal and subduction zone environments. Terra Nova http://dx.doi.org/10.1111/j.1365-3121.2011.00995.x.

Deschamps, F., Godard, M., Guillot, S., Chauvel, C., Andréani, M., Hattori, K., Wunder, B., France, L., 2012. Behavior of fluid-mobile elements in serpentines from abyssal to subduction environments: examples from Cuba and Dominican Republic. Chem. Geol. 313, 93–117.

Deschamps, F., Godard, M., Guillot, S., Hattori, K.H., 2013. Geochemistry of subduction zones serpentinites: a review. Lithos http://dx.doi.org/10.1016/j.lithos.2013.05.019.

DeShon, H.R., Schwartz, S.Y., 2004. Evidence for serpentinization of the forearc mantle wedge along the Nicoya Peninsula, Costa Rica. Geophys. Res. Lett. 31, L21611. http://dx.doi.org/10.1029/2004GL021179.

Detrick, R.S., White, R.S., Purdy, G.M., 1993. Crustal structure of North-Atlantic fracture zones. Rev. Geophys. 31, 439–459.

Dick, H.J.B., 1989. Abyssal peridotites, very slow spreading ridges and ocean ridge magmatism. In: Saunders, A.D., Norry, M.J. (Eds.), Magmatism in the Ocean Basins. Geological Society Special Publications 42, pp. 71–105.

Dorbath, C., Gerbault, M., Carlier, G., Guiraud, M., 2008. Double seismic zone of the Nazca plate in northern Chile: high-resolution velocity structure, petrological implications, and thermomechanical modeling. Geochem. Geophys. Geosyst. Q07006 http://dx.doi.org/10.1029/2008GC002020.

Escartín, J., Hirth, G., Evans, B., 1997. Nondilatant brittle deformation of serpentinites: implications for Mohr–Coulomb theory and the strength of faults. J. Geophys. Res. B 102, 2897–2913.

Escartin, J., Hirth, G., Evans, B., 2001. Strength of slightly serpentinized peridotites: implications for the tectonics of oceanic lithosphere. Geology 29, 1023–1026.

Escartín, J., Mevel, C., MacLeod, C., McCaig, A., 2003. Constraints on deformation conditions and the origin of oceanic detachments: the Mid-Atlantic Ridge core complex at 15°45′N. Geochem. Geophys. Geosyst. 4, 1–37. http://dx.doi.org/10.1029/2002GC000472.

Escartín, J., Andreani, M., Hirth, G., Evans, B., 2008. Relationships between the microstructural evolution and the rheology of talc at elevated pressures and temperatures. Earth Planet. Sci. Lett. 268 (463–475), 2008.

Evans, B.W., 2004. The serpentinite multisystem revisited: chrysotile is metastable. Int. Geol. Rev. 46, 479–506.

Evans, B.W., Hattori, K.H., Baronnet, A., 2013. Serpentinite: what, why, where? Elements 9, 99–106. http://dx.doi.org/10.2113/gselements.9.2.99.

Faulkner, D.R., Rutter, E.H., 2001. Can the maintenance of overpressured fluids in large strike-slip fault zones explain their apparent weakness? Geology 29, 503–506.

Faccenda, M., Gerya, T.V., Burlini, L., 2009. Deep slab hydration induced by bending related variations in tectonic pressure. Nature Geoscience 2, 790–793.

Federico, L., Crispini, L., Scambelluri, M., Capponi, G., 2007. Ophiolite mélange zone records exhumation in a fossil subduction channel. Geology 35, 499–502.

Festa, A., Pini, G.A., Dilek, Y., Codegone, G., Vezzani, L., Ghisetti, F., Lucente, C., Ogata, K., 2010. Peri-Adriatic meacutelanges and their evolution in the Tethyan realm. Int. Geol. Rev. 52, 369–403.

Florineth, D., Froitzheim, N., 1994. Transition from continental to oceanic basement in the Tasna nappe (Engadine window, Graubünden, Switzerland): evidence for Early Cretaceous opening of the Valais Ocean. Schweiz. Mineral. Petrogr. Mitt. 74, 437–448.

Früh-Green, G.L., Weissert, H., Bernoulli, D.E., 1990. A multiple fluid history recorded in alpine ophiolites. J. Geol. Soc. Lond. 147, 959–970.

Fryer, P., 1992. A synthesis of Leg 125 drilling of serpentine seamounts on the Mariana and Izu-Bonin forearcs. Ocean Drill. Program Sci. Results Leg 125, 593–614.

Fryer, P., Wheat, C.G., Mottl, M.J., 1999. Mariana Blueschist mud volcanism: implications for conditions within the subduction zone. Geology 27, 103–106.

Fryer, P., Gharib, J., Ross, K., Savov, I., Mottl, M.J., 2006. Variability in serpentine mudflow mechanisms and sources: OPD drilling results on Mariana forearc seamounts. Geochem. Geophys. Geosyst. 7. http://dx.doi.org/10.1029/2005GC001201.

Gasc, J., Schubnel, A., Brunet, F., Guillon, S., Mueller, H.J., Lathe, C., 2011. Simultaneous acoustic emissions monitoring and synchrotron X-ray diffraction at high pressure and temperature: calibration and application to serpentinite dehydration. Phys. Earth Planet. Inter. 189, 121–133.

Gerya, T.V., Stockhert, B., Perchuk, A.L., 2002. Exhumation of high-pressure metamorphic rocks in a subduction channel — a numerical simulation. Tectonic 21 (6), 1056. http://dx.doi.org/10.1029/2002TC001406.

Gerya, T.V., Connolly, J.A.D., Yuen, D.A., 2008. Why is terrestrial subduction one-sided? Geology 36, 43–46.

Gorczyk, W., Guillot, S., Gerya, T.V., Hattori, K.H., 2007. Asthenospheric upwelling, oceanic slab retreat and exhumation of UHP mantle rocks: insights from Greater Antilles. Geophys. Res. Lett. 34, L21309. http://dx.doi.org/10.1029/2007GL031059.

García-Casco, A., Torres-Roldán, R.L., Iturralde-Vinent, M.A., Millán, G., Núñez Cambra, K., Lázaro, C., Rodríguez Vega, A., 2006. High pressure metamorphism of ophiolites in Cuba. Geologica Acta 4, 63–88.

Gratier, J.P., Richard, J., Renard, F., Mittempergher, S., Doan, M.L., Di Toro, G., Hadizadeh, J., Boullier, A.M., 2011. Aseismic sliding of active faults by pressure solution creep: evidence from the San Andreas Fault Observatory at Depth. Geology http://dx.doi.org/10.1130/G32073.1.

Gueydan, F., Précigout, J., 2014. Mode of continental rifting as a function of ductile strain localization in the lithospheric mantle. Tectonophysics 612–613, 18–25.

Guillot, S., Hattori, K., 2013. Serpentinites: key roles in geodynamics, arc volcanoes, sustainable development and the origin of life. Elements 9, 95–98.

Guillot, S., Hattori, K., de Sigoyer, J., 2000. Mantle wedge serpentinization and exhumation of HP rocks: insights from Eastern Ladakh. Geology 28, 199–202.

Guillot, S., Hattori, K.H., de Sigoyer, J., Nägler, T., Auzende, A.L., 2001. Evidence of hydration of the mantle wedge and its role in the exhumation of eclogites. Earth Planet. Sci. Lett. 193, 115–127.

Guillot, S., Hattori, K.H., Agard, P., Schwartz, S., Vidal, O., 2009. Exhumation processes in oceanic and continental subduction contexts: a review. In: Lallemand, S., Funiciello, F. (Eds.), Subduction Zone Dynamics. Springer-Verlag, Berlin Heidelberg, pp. 175–204.

Hacker, B.R., Gerya, T.V., Gilotti, J.A., 2013. Formation and exhumation of ultrahigh-pressure terranes. Elements http://dx.doi.org/10.2113/gselements.9.4.289.

Hansen, L.N., Cheadle, M.J., John, B.E., Swapp, S.M., Dick, H.J.B., Tucholke, B.E., Tivey, M.A., 2013. Mylonitic deformation at the Kane oceanic core complex: implications for the rheological behavior of oceanic detachment faults. Geochem. Geophys. Geosyst. 14, 3085–3108.

Harlow, G.E., Hemming, S.R., Avé Lallemant, H.G., Sisson, V.B., 2004. Two high-pressure–low-temperature serpentinite-matrix mélange belts, Motagua fault zone, Guatemala: a record of Aptian and Maastrichtian collisions. Geology 32, 17–20.

Hattori, K., Guillot, S., 2003. Volcanic fronts as a consequence of serpentinite dehydration in mantle wedge. Geology 31, 525–528.
Hattori, K.H., Guillot, S., 2007. Geochemical character of serpentinites associated with high- to ultrahigh-pressure metamorphic rocks in the Alps, Cuba, and the Himalayas: recycling of elements in subduction zones. Geochem. Geophys. Geosyst. 8, Q09010 (0.1029/2007GC001594).
Hebert, R., Adamson, A.C., Komor, S.C., 1990. Metamorphic petrology of ODP leg 109, Hole 670A serpentinized peridotites: serpentinization processes at slow spreading ridge environment. Proc. Ocean Drill. Program Sci. Results 106 (109), 103–115.
Hébert, R., Gueddari, K., Lafléche, M.R., Beslier, M.O., Gardien, V., 2001. Petrology and geochemistry of exhumed peridotites and gabbros from non-volcanic margins: ODP Leg 173 West Iberia ocean–continent transition zone. In: Wilson, R.C.L., Whitmarsh, R.B., Taylor, B., Froitzheim, N. (Eds.), Non-volcanic Rifting of Continental Margins: A Comparison of Evidence From Land.
Helmstaedt, H., Sculze, D.J., 1988. Garnet clinopyroxenite–chlorite eclogite transition in a xenolith from Moses Rock: further evidence for metmorphosed ophiolites under the Colorado Plateau. In: Boyd, F.R., Meyer, H.O.A. (Eds.), The Mantle Sample: Inclusions in Kimberlites and Other Volcanics. American Geophysical Union, Washington, DC, pp. 357–373.
Hermann, J., Muntener, O., Scambelluri, M., 2000. The importance of serpentinite mylonites for subduction and exhumation of oceanic crust. Tectonophysics 327, 225–238.
Hess, H.H., 1955. Serpentines, orogeny and epeirogeny. Geochem. Soc. Spec. Publ. 62, 391–408.
Hess, H.H., 1962. History of ocean basins. In: Engel, A.E.J., James, H.L., Leonard, B.F. (Eds.), Petrologic Studies, The Burlington Volume. Geological Society of America, Boulder, CO, pp. 599–620.
Hilairet, N., Reynard, B., 2009. Stability and dynamics of serpentinite layer in subduction zone. Tectonophysics 465, 24–29.
Hilairet, N., Daniel, I., Reynard, B., 2006. P–V equations of state and the relative stabilities of serpentine varieties. Phys. Chem. Miner. 33, 629–637.
Hilairet, N., Reynard, B., Wang, Y., Daniel, I., Merkel, S., Nishiyama, N., Petitgirard, S., 2007. High-pressure creep of serpentine, interseismic deformation, and initiation of subduction. Science 318, 1910–1913.
Hirauchi, K., Michibayashi, K., Ueda, H., Katayama, I., 2010. Spatial variations in antigorite fabric across a serpentinite subduction channel: insights from the Ohmachi Seamount, Izu Bonin frontal arc. Earth Planet. Sci. Lett. 299, 196–206.
Hirth, G., Guillot, S., 2013. Rheology and tectonic significance of serpentinite. Elements 9, 107–113.
Hoogerduijn Strating, E.H., Rampone, E., Piccardo, G.B., Drury, M.R., 1993. Subsolidus emplacement of mantle peridotites during incipient oceanic rifting and opening of the Mesozoic Tethys (Voltri Massif, NW Italy). J. Petrol. 34, 901–927.
Hopper, J.R., Funck, T., Tucholke, B.E., Louden, K.E., Holbrook, W.S., Larsen, H.C., 2006. A deep seismic investigation of the Flemish Cap margin: implications for the origin of deep reflectivity and evidence for asymmetric breakup between Newfoundland and Iberia. Geophys. J. Inter. 164, 501–515.
Horen, H., Zamora, M., Dubuisson, G., 1996. Seismic waves velocities and anisotropy in serpentinized peridotites from xigaze ophiolite: abundance of serpentine in slow spreading ridge. Geophys. Res. Lett. 23, 9–12.
Huismans, R., Beaumont, C., 2012. Depth-dependent extension, two-stage breakup and cratonic underplating at rifted margins. Nature 473, 74–78.
Hyndman, R.D., Peacock, S.M., 2003. Serpentinization of the forearc mantle. Earth and Planet Science Letters 212, 417–432.
Ildefonse, B., Blackman, D.K., John, B.E., Ohara, Y., Miller, D.J., MacLeod, C.J., 2007. Oceanic core complexes and crustal accretion at slow-spreading ridges. Geology 35, 623–626.
Jammes, S., Manatschal, G., Lavier, L., Masini, E., 2009. Tectonosedimentary evolution related to extreme crustal thinning ahead of propagating ocean: example of the western Pyrenees. Tectonics 28. http://dx.doi.org/10.1029/2008TC002406.
Ji, S., Li, A., Wang, Q., Long, C., Wang, H., Marcotte, D., Salisbury, M., 2013. Seismic velocities, anisotropy, and shear-wave splitting of antigorite serpentinites and tectonic implications for subduction zones. J. Geophys. Res. 118, 1015–1037.
Jung, H., 2011. Seismic anisotropy produced by serpentine in mantle wedge. Earth Planet. Sci. Lett. 307, 535–543.
Jung, H., Green II, H.W., Dobrzhinetskaya, L.F., 2004. Intermediate-depth earthquake faulting by dehydration embrittlement with negative volume change. Nature 428, 545–549.
Kaczmarek, M.-A., Müntener, O., 2008. Juxtaposition of melt migration and high temperature shear zones in the upper mantle. Field and petrological constraints from the Lanzo peridotite (N-Italy). J. Petrol. 49, 2187–2220.
Kaczmarek, M.-A., Müntener, O., Rubatto, D., 2008. Trace element chemistry and U–Pb dating of zircons oceanic gabbros and their relationship with whole rock composition (Lanzo, Italian Alps). Contrib. Mineral. Petrol. 155, 295–312.
Kamimura, A., Kasahara, J., Shinohara, M., Hino, R., Shiobara, H., Fujie, G., Kanazawa, T., 2002. Crustal structure study at the Izu-Bonin subduction zone around 31 degrees N: implications of serpentinized materials along the subduction plate boundary. Phys. Earth Planet. Inter. 132, 105–129.
Karabacak, V., Altunel, E., Cakir, Z., 2011. Monitoring aseismic surface creep along the North Anatolian Fault (Turkey) using ground-based LIDAR. Earth Planet. Sci. Lett. 304, 64–70.
Karato, S.I., Paterson, M.S., Fitzgerald, J.D., 1986. Rheology of synthetic olivine aggregates: influence of grain size and water. J. Geophys. Res. 91, 8151–8176.
Karson, J.A., Fruh-Green, G.L., Kelley, D.S., Williams, E.A., Yoerger, D.R., Jakuba, M., 2006. Detachment shear zone of the Atlantis Massif core complex, Mid-Atlantic Ridge, 30 degrees N. Geochem. Geophys. Geosyst. 7. http://dx.doi.org/10.1029/2005GC001109.
Katayama, I., Hirauchi, K.-I., Michibayashi, K., Ando, J.I., 2009. Trench-parallel anisotropy produced by serpentine deformation in the hydrated mantle wedge. Nature 461, 1114–1117.
Kawakatsu, H., Watada, S., 2007. Seismic evidence for deep-water transportation in the mantle. Science 316, 1468–1471.
Kelemen, P.B., Hirth, G., 2007. A periodic shear-heating mechanism for intermediate depth earthquakes in the mantle. Nature 446, 787–790.
Kelley, D.S., et al., 2001. An off-axis hydrothermal vent field discovered near the Mid-Atlantic Ridge at 30°N. Nature 412, 145–149.
King, S.D., 2001. Subduction zones: observations and geodynamic models. Phys. Earth Planet. Inter. 127, 9–24. http://dx.doi.org/10.1016/S0031-9201(01)00218-7.
Kirby, S., Uno, M., 2013. Evidence for multi-stage infiltration of aqueous fluids in a block-emplaced serpentinite along the San Andreas Fault system, Redwood City, California. Japan Geosciences Union Meeting Abstracts ST06-16, Chiba, Japan.
Kirby, S.H., Wang, K., Brocher, T.M., 2014. A large mantle water source for the northern San Andreas Fault system: a ghost of subduction past. Earth, Planets and Space 66–67. http://dx.doi.org/10.1186/1880-5981-66-67.
Kohli, A.H., Goldsby, D.L., Hirth, G., Tullis, T., 2011. Flash weakening of serpentinite at near-seismic slip rates. J. Geophys. Res. 116. http://dx.doi.org/10.1029/2010JB007833.
Kohlstedt, D.L., Evans, B., Mackwell, S.J., 1995. Strength of the lithosphere: constraints imposed by laboratory experiments. J. Geophys. Res. 100 (17), 17–587 (602).
Krebs, M., Schertl, H.P., Maresch, W.V., Draper, G., 2011. Mass flow in serpentinite-hosted subduction channels: P–T–t path patterns of metamorphic blocks in the Rio San Juan mélange (Dominican Republic). J. Asian Earth Sci. 42, 569–595.
Lagabrielle, Y., Bodinier, J.L., 2008. Submarine reworking of exhumed subcontinental mantle rocks: field evidence from the Lherz peridotites, French Pyrenees. Terra Nova 20, 11–21.
Lagabrielle, Y., Cannat, M., 1990. Alpine Jurassic ophiolites resemble the modern central. Atl. Basement Geol. 18, 319–322.
Lagabrielle, Y., Labaume, P., de Saint Blanquat, M., 2010. Mantle exhumation, crustal denudation, and gravity tectonics during Cretaceous rifting in the Pyrenean realm (SW Europe): insights from the geological setting of the lherzolite bodies. Tectonics 29. http://dx.doi.org/10.1029/2009TC002588.
Le Roux, V., Bodinier, J.-L., Tommasi, A., Alard, O., Dautria, J.-M., Vauchez, A., Riches, A.J.V., 2007. The Lherz spinel lherzolite: refertilized rather than pristine mantle. Earth Planet. Sci. Lett. 259, 599–612.
Lefeldt, M., Grevemeyer, I., Gossler, J., Bialas, J., 2009. Intraplate seismicity and related mantle hydration at the Nicaraguan trench outer rise. Geophys. J. Int. 178, 742–752.
Lefeldt, M., Ranero, C.R., Grevemeyer, I., 2012. Seismic evidence of tectonic control on the depth of water influx into incoming oceanic plates at subduction trenches. Geochemistry, Geophysics, Geosystems 13 Q05013.
Lemoine, M., Tricart, P., Boillot, G., 1987. Ultramafic and gabbroic ocean floor of the Ligurian Tethys (Alps, Corsica, Apennines): in search of a genetic model. Geology 15, 622–625.
Lewis, J.F., Draper, G., Proenza, J.A., Espaillat, J., Jiménez, J., 2006. Ophiolite-related ultramafic rocks (serpentinites) in the Caribbean region: a review of their occurrence, composition, origin, emplacement and Ni-laterite soil formation. Geol. Acta 4, 237–263.
Li, X.P., Rahn, M., Bucher, K., 2004. Serpentinites of the Zermatt–Saas ophiolite complex and their texture evolution. J. Metamorph. Geol. 22, 159–177.
Liou, J.G., Hacker, B.R., Zhang, R.Y., 2000. Into the forbidden zone. Science 287, 1215–1216.
Lombardo, B., Nervo, R., Compagnoni, R., et al., 1978. Osservazioni preliminari sulle ofioliti metamorfiche del Monviso (Alpi occidentali). Rend. Soc. Ital. Mineral. Petrol. 34, 253–305.
MacLeod, C.J., Escartín, J., Banerji, D., Banks, G.J., Gleeson, M., Irving, D.H.B., Lilly, R.M., McCaig, A., Niu, Y.-L., Allerton, S., Smith, D.K., 2002. Direct geological evidence for oceanic detachment faulting: the Mid-Atlantic Ridge, 15 45°N. Geology 30, 279–282.
Malatesta, C., Crispini, L., Federico, L., Capponi, G., Scambelluri, M., 2012. The exhumation of high pressure ophiolites (Voltri Massif, Western Alps): insights from structural and petrologic data on metagabbro bodies. Tectonophysics 568-569, 102–133.
Malvoisin, B., Brunet, F., Carlut, J., Rouméjon, S., Cannat, M., 2012. Serpentinization of oceanic peridotites: 2. Kinetics and processes of San Carlos olivine hydrothermal alteration. J. Geophys. Res. 117. http://dx.doi.org/10.1029/2011JB008842.
Manaker, D.M., Calais, E., Freed, A.M., Ali, S.T., Przybylski, P., Mattioli, G., Jansma, P., de Prepetit, C., Chabalier, J.B., 2008. Seismology interseismic plate coupling and strain partitioning in the northeastern Caribbean. Geophys. J. Inter. 174, 889–903.
Manatschal, G., Müntener, O., 2009. A type sequence across an ancient magma-poor ocean–continent transition: the example of the western Alpine Tethys ophiolites. Tectonophysics 473, 4–19.
Manatschal, G., Engstrom, A., Desmurs, L., Schaltegger, U., Cosca, M., Müntener, O., Bernoulli, D., 2006. What is the tectono-metamorphic evolution of continental break-up: the example of the Tasna Ocean–Continent transition. J. Struct. Geol. 28, 1849–1869.
Mével, C., 2003. Serpentinization of abyssal peridotites at mid-ocean ridges. C. R. Geosci. 335, 825–852.
Mével, C., Cannat, M., Gente, P., Marion, E., Auzende, J.M., Karson, J.A., 1991. Emplacement of deep crustal and mantle rocks on the west median valley wall of the MARK area (MAR 23°N). Tectonophysics 190, 31–53.
Minshull, T.A., 2009. Geophysical characterisation of the ocean–continent transition at magma-poor rifted margins. C. R. Geosci. 341, 382–393. http://dx.doi.org/10.1016/j.crte.2008.09.003.
Mohn, G., Manatschal, G., Beltrando, M., Masini, E., Kusznir, N., 2012. Necking of continental crust in magma-poor rifted margins: evidence from the fossil Alpine Tethys margins. Tectonics 31, TC1012. http://dx.doi.org/10.1029/2011TC002961.
Moore, D.E., Rymer, M.J., 2007. Talc bearing serpentinite and the creeping section of the San Andreas Fault. Nature 448, 795–797. http://dx.doi.org/10.1038/nature06064.
Moore, D.E., Rymer, M.J., 2011. Frictional strengths of talc-serpentine and talc-quartz mixtures. J. Geophys. Res. 116, B01403. http://dx.doi.org/10.1029/2010JB007881.

Moore, D.E., Lockner, D.A., Summers, R., Shengli, M.A., Byerlee, J.D., 1996. Strengths of chrysotile-serpentinite gouge under hydrothermal conditions: can it explain a weak San Andreas fault? Geology 24, 1041–1044.
Moore, D.E., Lockner, D.A., Iwata, K., Dhengli, M., Summers, R., Byerlee, J.D., 1997. Strengths of serpentinite gouges at elevated temperatures. J. Geophys. Res. 102, 14787–14801.
Moore, D., Lockner, D., Tanaka, H., Iwata, K.C., 2004. Coefficient of friction of chrysotile gouge at seismogenic depths. Int. Geol. Rev. 46 (5), 385–398.
Morrow, C.A., Moore, D.E., Lockner, D.A., 2000. The effect of mineral bond strength and adsorbed water on fault gouge frictional strength. Geophys. Res. Lett. 27, 815–818.
Mouthereau, F., Watts, A.B., Burov, E., 2013. Structure of orogenic belts controlled by lithosphere age. Nat. Geosci. 6, 785–789.
Müntener, O., Manatschal, G., 2006. High degrees of melt extraction recorded by spinel harzburgite of the Newfoundland margin: the role of inheritance and consequences for the evolution of the southern North Atlantic. Earth Planet. Sci. Lett. 252, 437–452. http://dx.doi.org/10.1016/j.epsl.2006.10.009.
Müntener, O., Hermann, J., Trommsdorff, V., 2000. Cooling history and exhumation of lower-crustal granulite and upper mantle (Malenco, Eastern Central Alps). J. Petrol. 41, 175–200.
Müntener, O., Pettke, T., Desmurs, L., Meier, M., Schaltegger, U., 2004. Refertilization of mantle peridotite in embryonic ocean basins: trace element and Nd isotopic evidence and implications for crust–mantle relationships. Earth Planet. Sci. Lett. 221, 293–308.
Müntener, O., Manatschal, G., Desmurs, L., Pettke, T., 2010. Plagioclase peridotites in ocean–continent transitions: refertilized mantle domains generated by melt stagnation in the shallow mantle lithosphere. J. Petrol. 51, 55–294.
Nakajima, J., Tsuji, Y., Hasegawa, A., Kita, S., Okada, T., Matsuzawa, T., 2009. Tomographic imaging of hydrated crust and mantle in the subducting Pacific slab beneath Hokkaido, Japan: evidence for dehydration embrittlement as a cause of intraslab earthquakes. Gondwana Res. 16, 470–481.
Nicholls, I.A., Ferguson, J., Jones, H., Marks, G.P., Mutter, J.C., 1981. Ultramafic blocks from the ocean floor southwest of Australia. Earth Planet. Sci. Lett. 56, 362–374.
Nicolas, A., Dupuy, C., 1984. Origin of ophiolitic and oceanic lherzolites. Tectonophysics 110, 177–187.
Nikulin, A., Levin, V., Park, J., 2009. Receiver function study of the Cascadia megathrust: evidence for localized serpentinization. Geochem. Geophys. Geosyst. 10, Q07004. http://dx.doi.org/10.1029/2009GC002376.
Nishii, A., Wallis, S.R., Mizukami, T., Michibayashi, K., 2012. Subduction related antigorite CPO patterns from forearc mantle in the Sanbagawa belt, southwest Japan. J. Struct. Geol. 33, 1436–1445.
Nozaka, T., Fryer, P., 2011. Alteration of he oceanic lower crust at a slow spreading axis: insight from vein-related zoned halos in olivine gabbro from Atlantis Massif, Mid-Atlantic Ridge. J. Petrol. 52, 643–664.
O'Hanley, D.S., 1996. Serpentinites: records of tectonic and petrological history. Oxf. Monogr. Geol. Geophys. 34, 277.
Padrón-Navarta, J.A., López Sánchez-Vizcaíno, V., Hermann, J., Connolly, J.A.D., Garrido, C.J., Gómez-Pugnaire, M.T., Marchesi, C., 2013. Tschermak's substitution in antigorite and consequences for phase relations and water liberation in high-grade serpentinites. Lithos 15, 186–196.
Peacock, S.M., 2001. Are the lower planes of double seismic zones caused by serpentine dehydration in subducting oceanic mantle? Geology 29, 299–302.
Peacock, S.M., Wang, K., 1999. Seismic consequences of warm versus cool subduction zone metamorphism: Examples from northeast and southwest Japan. Science 286, 937–939.
Pera, E., Mainprice, D., Burlini, L., 2003. Anisotropic seismic properties of the upper mantle beneath the Torre Alfina area (Northern Appennines, Central Italy). Tectonophysics 370, 11–30.
Péron-Pinvidic, G., Manatschal, G., 2009. The final rifting evolution at deep magma-poor passive margins from Iberia–Newfoundland: a new point of view. Int. J. Earth Sci. 98, 1581–1597.
Perrillat, J.P., Daniel, I., Koga, K.T., Reynard, B., Cardon, H., Crichton, W.A., 2005. Kinetics of antigorite dehydration: a real-time X-ray diffraction study. Earth Planet. Sci. Lett. 236, 899–913.
Picazo, S., Manatschal, G., Cannat, M., Andreani, M., 2013. Deformation associated to exhumation of serpentinized mantle rocks in a fossil ocean continent transition: the Totalp unit in SE Switzerland. Lithos 176, 255–271.
Piccardo, G.B., Vissers, R.L.M., 2007. The pre-oceanic evolution of the Erro–Tobbio peridotite (Voltri Massif, Ligurian Alps, Italy). J. Geodyn. 43, 417–449.
Piccardo, G.B., Müntener, O., Zanetti, A., Pettke, T., 2004. Ophiolitic peridotites of the Alpine–Apennine system: mantle processes and geodynamic relevance. Int. Geol. Rev. 46, 1119–1159.
Précigout, J., Gueydan, F., 2009. Mantle weakening and strain localization: implications for the long-term strength of the continental lithosphere. Geology 37, 147–150.
Raleigh, C.B., Paterson, M.S., 1965. Experimental deformation of serpentinite and its tectonic implications. J. Geophys. Res. 70, 3965–3985.
Ramachandran, K., Hyndman, R.D., 2012. The fate of fluids released from subducting slab in Northern Cascadia. Solid Earth 3, 121–129.
Rampone, E., 2004. Mantle dynamics during Permo-Mesozoic extension of the Europe-Adria lithosphere: insights from the Ligurian ophiolites. Periodico di Mineralogia 73, 215–230.
Rampone, E., Hofmann, A.W., Piccardo, G.B., Vannucci, R., Bottazzi, P., Ottolini, L., 1995. Petrology, mineral and isotope geochemistry of the external Liguride peridotites (Northern Apennines, Italy). J. Petrol. 36, 81–105.
Ramsay, J.G., Huber, M.I., 1987. The Techniques of Modern Structural Geology 2. 3 ed. Academic Press, p. 392.
Ranero, C.R., Sallares, V., 2004. Geophysical evidence for hydration of the crust and mantle of the Nazca plate during bending at the north Chile trench. Geology 32, 549–552.
Ranero, C.R., Morgan, J.P., McIntosh, K., Reichert, C., 2003. Bending-related faulting and mantle serpentinization at the Middle America trench. Nature 425, 367–373.
Reinen, L.A., Weeks, J.D., Tullis, T.E., 1994. The frictional behavior of lizardite and antigorite serpentinites: experiments, constitutive models, and implications for natural faults. Pure Appl. Geophys. 143, 317–358.
Reston, T.J., Krawczyk, C.M., Klaeschen, D., 1996. The S reflector west of Galicia (Spain): evidence from prestack depth migration for detachment faulting during continental breakup. J. Geophys. Res. 101, 8075–8091.
Reynard, B., 2013. Serpentine in active subduction zones. Lithos 178, 171–185.
Reynard, B., Nakajima, J., Kawakatsu, H., 2010. Earthquakes and plastic deformation of anhydrous slab mantle in double Wadati–Benioff zones. Geophys. Res. Lett. 37, L24309.
Robertson, A.H.F., 2007. Evidence of continental breakup from the Newfoundland Rifted Margin (Ocean Drilling Program Leg 210): lower Cretaceous seafloor formed by exhumation of subcontinental mantle lithosphere and the transition to seafloor spreading. In: Tucholke, B.E., Sibuet, J.-C. (Eds.), Scientific Results. Ocean Drilling Program. Texas A&M University, College Station, TX, pp. 1–69.
Roumejeon, S., Cannat, M., 2014. Serpentinization of mantle-derived peridotites at mid-ocean ridges: mesh texture development in the context of tectonic exhumation. Geochem. Geophys. Geosyst. http://dx.doi.org/10.1002/2013GC005148.
Rupke, L., Morgan, J.P., Hort, M., Connolly, J.A.D., 2004. Serpentine and the subduction zone water cycle. Earth Planet. Sci. Lett. 223, 17–34.
Saumur, B.M., Hattori, K., Guillot, S., 2010. Serpentinized abyssal and forearc peridotites in northern Dominican Republic: HP–LT mélange formation and protrusion along major strike-slip faults in an oceanic subduction complex. Geol. Soc. Am. Bull. http://dx.doi.org/10.1130/B26530.1.
Sauter, D., Cannat, M., Rouméjon, S., Andreani, M., Birot, D., Bronner, A., Brunelli, D., Carlut, J., Delacour, A., Guyader, V., MacLeod, C., Manatschal, G., Mendel, V., Ménez, B., Pasini, V., Ruellan, E., Searle, R., 2013. Continuous exhumation of mantle derived-rocks at the Southwest Indian Ridge for 11 million years. Nat. Geosci. 6, 314–320.
Scambelluri, M., Phillippot, P., 2001. Deep fluids in subduction zones. Lithos 55, 213–227.
Scambelluri, M., Tonarini, S., 2012. Boron isotope evidence for shallow fluid transfer across subduction zones by serpentinized mantle. Geology 40. http://dx.doi.org/10.1130/G33233.1.
Scambelluri, M., Muntener, O., Hermann, J., Piccardo, G.B., Trommsdorff, V., 1995. Subduction of water into the mantle: history of an alpine peridotite. Geology 23, 459–462.
Schleicher, A.M., van der Pluijm, B.A., Warr, L.N., 2010. Nanocoatings of clay and creep of the San Andreas fault at Parkfield, California. Geology 3, 667–670.
Schulz, S.S., Mavko, G.M., Burford, R.O., Stewart, W.D., 1982. Long-term fault creep observations in central California. J. Geophys. Res. 87, 6977–6982.
Schwartz, S., Lardeaux, J.M., Guillot, S., Tricart, P., 2000. The diversity of eclogitic metamorphism in the Monviso ophiolitic complex, western Alps, Italy. Geodin. Acta 13, 169–188.
Schwartz, S., Allemand, P., Guillot, S., 2001. Numerical model of the effect of serpentinites on the exhumation of eclogitic rocks: insights from the Monviso ophiolitic massif (Western Alps). Tectonophysics 342, 193–206.
Schwartz, S., Guillot, S., Reynard, B., Lafay, R., Nicollet, C., Debret, B., Auzende, A.L., 2013. Pressure–temperature estimates of the lizardite/antigorite transition in high pressure serpentinites. Lithos 178, 197–210.
Shreve, R.L., Cloos, M., 1986. Dynamics of sediment subduction, melange formation and prism accretion. Journal of Geophysical Research 91, 10 229–10 245.
Sengör, A.M.C., Tuysuz, O., Imren, C., 2005. The North Anatolian Fault: a new look. Annu. Rev. Earth Planet. Sci. 33, 37–112.
Skelton, A.D.L., Valley, J.W., 2000. The relative timing of serpentinisation and mantle exhumation at the ocean–continent transition, Iberia: constraints from oxygen isotopes. Earth Planet. Sci. Lett. 178, 327–338.
Smith, D., 2010. Antigorite peridotite, metaserpentinite, and other inclusions within diatremes on the Colorado Plateau, SW USA: implications for the mantle wedge during low-angle subduction. J. Petrol. 51, 1355–1379.
Smith, D.K., Cann, J.R., Escartin, J., 2006. Widespread active detachment faulting and core complex formation near 13 degrees N on the Mid-Atlantic Ridge. Nature 442, 440–443.
Song, T.R.A., Helmberger, D.V., Brudzinski, M.R., Clayton, R.W., Davis, P., Perez-Campos, X., Singh, S.K., 2009. Subducting slab ultra-slow velocity layer coincident with silent earthquakes in Southern Mexico. Science 324, 502–506.
Steinmann, G., 1905. Geologische Beobachtungen in den Alpen, II. Die Schardtsche Ueberfaltungstherorie und die geologische Bedeutung der Tiefseeabsätze und der ophiolitihischen Massengesteine. Berichte der Naturforschenden Gesellschaft zu Freiburg im Breisgau 16, 18–67.
Strating, E.H.H., Vissers, R.L.M., 1991. Dehydration-induced fracturing of eclogite-facies peridotites — implications for the mechanical-behavior of subducting oceanic lithosphere. Tectonophysics 200, 187–198.
Sutra, E., Manatschal, G., 2012. How does the continental crust thin in a hyper-extended rifted margin? Insights from the Iberia margin. Geology 40, 139–142. http://dx.doi.org/10.130/G32786.1.
Sutra, E., Manatschal, G., Mohn, G., Unternehr, P., 2013. Quantification and restoration of extensional deformation along the Western Iberia and Newfoundland rifted margins. Geochem. Geophys. Geosyst. 14, 2575–2597.
Syracuse, E.M., van Keken, P.E., Abers, G.A., 2010. The global range of subduction zone thermal models. Phys. Earth Planet. Inter. 183, 73–90.
Tackley, P.J., 2000. Self-consistent generation of tectonic plates in time-dependent, three dimensional mantle convection simulations. Geochem. Geophys. Geosyst. 1. http://dx.doi.org/10.1029/2002JB001918.
Tapponnier, P., Peltzer, G., Le Dain, Y., Armijo, R., Cobbold, P., 1982. Propagating extrusion tectonics in Asia: new insights from simple experiments with plasticine. Geology 10, 611–616.

Teyssier, C., Tikoff, B., 1998. Strike-slip partitioned transpression of the San Andreas Fault system: a lithospheric-scale approach. Geol. Soc. Lond. Spec. Publ. 135, 143–158.
Tibi, R., Wiens, D.A., Yuan, X.H., 2008. Seismic evidence for widespread serpentinized forearc mantle along the Mariana convergence margin. Geophys. Res. Lett. 35, L13303. http://dx.doi.org/10.1029/2008gl034163.
Tilmann, F., Flueh, E., Planert, L., Reston, T., Weinrebe, W., 2004. Microearthquake seismicity of the Mid-Atlantic Ridge at 5°S: a view of tectonic extension. J. Geophys. Res. 109, B06102. http://dx.doi.org/10.1029/2003JB002827.
Tommasi, A., Godard, M., Coromina, G., Dautria, J.-M., Barsczus, H.G., 2004. Seismic anisotropy and compositionally induced velocity anomalies in the lithosphere above mantle plumes: a petrological and microstructural study of mantle xenoliths from French Polynesia. Earth Planet. Sci. Lett. 227, 539–556.
Toomey, D.R., Purdy, G.M., Solomon, S.C., 1988. Microearthquakes beneath the median valley of the Mid-Atlantic Ridge near 23°N: tomography and tectonics. J. Geophys. Res. 93, 9093–9112.
Tsujimori, T., Liou, J.G., Coleman, R.G., 2007. Finding of high-grade tectonic blocks from the New Idria serpentinite body, Diablo Range, California: petrologic constraints on the tectonic evolution of an active serpentinite diapir. Geol. Spec. Pap. 419, 67–80.
Tucholke, B.E., Sibuet, J.-C., 2007. Leg 210 synthesis: tectonic, magmatic, and sedimentary evolution of the Newfoundland–Iberia rift. In: Tucholke, B.E., Sibuet, J.-C., Klaus, A. (Eds.), Proceedings ODP, Scientific Results, 210. Ocean Drilling Program, College Station, TX, pp. 1–56 http://dx.doi.org/10.2973/odp.proc.sr.210.101.2007.
Ulmer, P., Trommsdorff, V., 1995. Serpentine stability to mantle depths and subduction-related magmatism. Science 268, 858–861.
Ulrich, M., Picard, C., Guillot, S., Chauvel, C., Cluzel, D., Meffre, S., 2010. Multiple melting stages and refertilization as indicators for ridge to subduction formation: the New Caledonia ophiolite. Lithos 115, 223–236.
Usui, T., Nakamura, E., Kobayashi, K., Mayurama, S., Helmstaedt, H., 2003. Fate of the subducted Farallon plate inferred from eclogite xenoliths from the Colorado Plateau. Geology 31, 589–592.
Van de Moortele, B., Bezacier, L., Trullenque, G., Reynard, B., 2010. Electron backscattering diffraction (EBSD) measurements of antigorite lattice-preferred orientations (LPO). J. Microsc. Oxford 239, 245–248.
Van Keken, P.E., Hacker, B.R., Syracuse, E.M., Abers, G.A., 2011. Subduction Factory: 4.
Wada, I., Wang, K.L., He, J.G., Hyndman, R.D., 2008. Weakening of the subduction interface and its effects on surface heat flow, slab dehydration, and mantle wedge serpentinization. J. Geophys. Res. Solid Earth 113.
Wallace, R.E., 1990. The San Andreas Fault system, California. USGS Professional Paper 1515, Washington (283 pp.).
Wallis, S.R., Kobayashi, H., Nishii, A., Mizukami, T., Seto, Y., 2011. Obliteration of olivine crystallographic preferred orientation patterns in subduction-related antigorite bearing mantle peridotite: an example from the Higashi–Akaishi body, SW Japan. In: Prior, D.J., Rutter, E.H., Tatham, D. (Eds.), Deformation Mechanisms, Rheology and Tectonics: Microstructures, Mechanics and Anisotropy. Special Publications. Geological Society, London, pp. 113–127.
Whitmarsh, R.B., Beslier, M.O., Wallace, P.J., 1998. Return to Iberia. Proceedings of the Ocean Drilling Program, Initial Reports. 173. Ocean Drilling Program, College Station, Tex.
Whitmarsh, R.B., Manatschal, G., Minshull, T.A., 2001. Evolution of magma-poor continental margins from rifting to seafloor spreading. Nature 413, 150–154.
Wunder, B., Schreyer, W., 1997. Antigorite: high-pressure stability in the system MgO–SiO2–H2O. Lithos 41, 213–227.
Yamasaki, T., Seno, T., 2003. Double seismic zone and dehydration embrittlement of the subducting slab. J. Geophys. Res. 108, 2212. http://dx.doi.org/10.1029/2002JB001918.
Zhao, D., 2004. Global tomographic images of mantle plumes and subducting slabs: insight into deep. Phys. Earth Planet. Inter. 146, 3–34. http://dx.doi.org/10.1016/j.pepi.2003.07.032.